AFRL-AFOSR-UK-TR-2012-0035

Laminar Flow Breakdown due to Particle Interactions

Conny M. Schmidt

University of Limerick
National Technological Park
MAE Dept, L1-023
Limerick, Ireland

EOARD Grant 11-3044

Report Date: August 2012

Final Report from 01 July 2011 to 29 February 2012

Distribution Statement A: Approved for public release distribution is unlimited.

Air Force Research Laboratory
Air Force Office of Scientific Research
European Office of Aerospace Research and Development
Unit 4515 Box 14, APO AE 09421

REPORT DOCUMENTATION PAGE

Form Approved OMB No. 0704-0188

Public reporting burden for this collection of information is estimated to average 1 hour per response, including the time for reviewing instructions, searching existing data sources, gathering and maintaining the data needed, and completing and reviewing the collection of information. Send comments regarding this burden estimate or any other aspect of this collection of information, including suggestions for reducing the burden, to Department of Defense, Washington Headquarters Services, Directorate for Information Operations and Reports (0704-0188), 1215 Jefferson Davis Highway, Suite 1204, Arlington, VA 22202-4302. Respondents should be aware that notwithstanding any other provision of law, no person shall be subject to any penalty for failing to comply with a collection of information if it does not display a currently valid OMB control number.
PLEASE DO NOT RETURN YOUR FORM TO THE ABOVE ADDRESS.

1. REPORT DATE *(DD-MM-YYYY)*	2. REPORT TYPE	3. DATES COVERED *(From – To)*
22 August 2012	Final Report	1 July 2011 – 29 February 2012

4. TITLE AND SUBTITLE

Laminar Flow Breakdown due to Particle Interactions

5a. CONTRACT NUMBER

FA8655-11-1-3044

5b. GRANT NUMBER

Grant 11-3044

5c. PROGRAM ELEMENT NUMBER

61102F

6. AUTHOR(S)

Conny M. Schmidt

5d. PROJECT NUMBER

5d. TASK NUMBER

5e. WORK UNIT NUMBER

7. PERFORMING ORGANIZATION NAME(S) AND ADDRESS(ES)

University of Limerick
National Technological Park
MAE Dept, L1-023
Limerick, Ireland

8. PERFORMING ORGANIZATION REPORT NUMBER

N/A

9. SPONSORING/MONITORING AGENCY NAME(S) AND ADDRESS(ES)

EOARD
Unit 4515 BOX 14
APO AE 09421

10. SPONSOR/MONITOR'S ACRONYM(S)

AFRL/AFOSR/RSW (EOARD)

11. SPONSOR/MONITOR'S REPORT NUMBER(S)

AFRL-AFOSR-UK-TR-2012-0035

12. DISTRIBUTION/AVAILABILITY STATEMENT

Approved for public release; distribution is unlimited. (approval given by local Public Affairs Office)

13. SUPPLEMENTARY NOTES

14. ABSTRACT

The principle mechanisms leading to the transition of a laminar boundary layer due to a small particle travelling through it are not well understood. Whereas, it is generally accepted that the effect can be attributed to the particles ability of producing turbulence within its wake, the critical parameters have not been experimentally verified until today. This report details an investigation into the breakdown of Laminar Flow.

15. SUBJECT TERMS

EOARD, laminnar flow, Aerodynamics, Boundary Layer

16. SECURITY CLASSIFICATION OF:			17. LIMITATION OF ABSTRACT	18, NUMBER OF PAGES	19a. NAME OF RESPONSIBLE PERSON
a. REPORT	b. ABSTRACT	c. THIS PAGE			Gregg Abate
UNCLAS	UNCLAS	UNCLAS	SAR	56	19b. TELEPHONE NUMBER *(Include area code)* +44 (0)1895 616021

Grant Number: FA8655-11-1-3044

Laminar Flow Breakdown due to Particle Interaction

Final Report

01/10/2011 – 15/08/2012

Conny Schmidt

approved by: Dr. Trevor Young,
trevor.young@ul.ie
Senior lecturer,
MABE department
University of Limerick
Ireland

author's details: Conny Schmidt,
conny.schmidt@ul.ie
PhD student,
MABE department,
University of Limerick
Ireland

Distribution A: Approved for public release; distribution is unlimited.

Table of Contents

Distribution A: Approved for public release; distribution is unlimited.

Distribution A: Approved for public release; distribution is unlimited.

List of Figures

Distribution A: Approved for public release; distribution is unlimited.

Distribution A: Approved for public release; distribution is unlimited.

Summary

The principle mechanisms leading to the transition of a laminar boundary layer due to a small particle travelling through it are not well understood. Whereas, it is generally accepted that the effect can be attributed to the particles ability of producing turbulence within its wake, the critical parameters have not been experimentally verified until today.

The great difficulties encountered during efforts to re-create the naturally occurring mechanisms in the laboratory have led to the proposal of an alternative experimental method. This is based on a surface moving within a fluid at rest, thus reversing the conventionally applied wind tunnel approach. It allows for a fixed positioning of the particle to be investigated, while the involved processes can be slowed down, thus alleviating the measurements to be taken.

A computational pre-study on the proposed method has generated encouraging results in terms of (1) time-limited boundary layer growth and (2) flow field stability. Nevertheless, some indication was given that thicker boundary layers should be expected when compared to those developing over a flat plate at zero pressure gradient conditions.

A physical realization of the proposed method has been manufactured. Preliminary tests have been successful in terms of obtaining a stable equilibrium of the generated non-uniform flow field. Measurements obtained from boundary layer Pitot tube traverses were found to be repeatable.

The tests also revealed that a certain amount of background flow is generally excited throughout the test section. Since, however, this appears to be slow, the particle conditions can easily be kept sub-critical within those regions. Furthermore, it could be shown that the background flow can be reduced by introducing a small pressure gradient. For the determined optimal configuration, a surprisingly close match of the velocity profile when compared to the Blasius profile has been obtained.

During attempts to obtain more accurate data from hot wire measurements unexpected problems were encountered. The signals of the employed single hot wire probes showed regular large amplitude disturbances which were exactly in line with the frequency of the rotating drum, and thus attributable to a slight imperfection of the manufactured test facility. An effort to improve the found concentricity deviation was successful in reducing the effect to within the developing boundary layer.

Meaningful visualizations of the particle's wake when immersed into the non-uniform flow field of the boundary layer proved to be difficult, since the smoke within the latter is quickly carried away. Outside of those regions the applied technique provided for clear representations, substantiating both a quasi-quiescent free stream and the boundary layer thickness as derived from Pitot traverses.

Despite of the issues met, the fabricated particle wake investigation facility is likely to produce some of the missing answers on the particle wake development within a wall-bounded non-uniform flow, subject to an upgrade of the currently employed measurement techniques (e.g. crossed HW probes or PIV).

Distribution A: Approved for public release; distribution is unlimited.

Introduction

Steadily increasing energy costs and a growing awareness of the environmental impact of the burning of fossil fuels have renewed R & D interest in laminar flow technologies in aeronautics. These technologies have the potential to considerably reduce the friction drag of eligible aircraft components by maintaining a laminar boundary layer state at chord positions that are conventionally associated with turbulent flow. Drag reductions in the order of 15% have been proposed to be realistic, which translates into a net benefit of up to 10% fuel savings. [1, 34, 41] This is an immense potential considering that across the airline industry $700 million per annum could be saved by lowering fuel consumption by as little as 1%. [12]

Whereas, most of the coherent technological challenges are reasonably well-understood, knowledge about operational aspects, such as, the effect on the boundary layer when encountering cirrus cloud, is incomplete. The observed performance degradations [5, 9] have been attributed to the ability of the ice crystals to produce turbulence within their wakes when entering the artificially-maintained laminar boundary layers [9]. Premature transition can be triggered by such turbulent contamination mechanisms.

While the main focus of this work lies in the aeronautical field, some considerations are also given to studies that were run under water.

Background

Aeronautical Applications

For an aircraft flying through a cirrus cloud the prevailing situation may be described as follows. The ice particles are typically very small in comparison to the dimensions of an aircraft component over which the affected laminar boundary layer is maintained by drag reduction techniques. Moreover, in the majority of cases, the particle dimensions will be an order of magnitude smaller than the boundary layer itself [9]. Furthermore, it may be acceptable to consider the ice crystals as being in equilibrium to the surrounding air before being approached by an aircraft, since their falling velocities will rarely exceed 2 m/s, whereas a typical cruise speed of a commercial jet transport is in the order of 200 m/s. At the same time the ratio of the density of the particles to that of the surrounding air is usually large (in the order of 10^3) when considering particles that are primarily composed of water. As earlier studies have concluded that the application of drag reduction technologies based on maintaining extended regions of laminar flow are limited in their practicability to altitudes above 20,000 ft [40], this may also be considered a valid assumption.

This results in a twofold effect. While on one hand, an approached ice crystal will quite closely follow the streamlines of the adjacent air (when being diverted around an aircraft wing for example)

Distribution A: Approved for public release; distribution is unlimited.

on the larger scale, its relatively heavy weight makes it impossible for the particle to adapt to the rapid velocity changes occurring within a boundary layer when entering it. This gives rise to the build-up of a relative velocity between the particle and the air that is large enough to enable the ice crystal to produce a wake while travelling through those regions. Subject to this wake containing turbulence it is widely accepted that transition of a laminar boundary layer could occur due to a turbulent contamination mechanism.

The X-21 flight tests and the "Hall Criteria" [9]

In the early 1960s, researchers at Northrop were the first to recognize that ice crystals as occurring in cirrus cloud would have a detrimental effect on the performance of Laminar Flow Control (LFC) systems. During flight tests of full chord suction type LFC systems aboard two X-21 aircraft, laminar flow was entirely lost when entering thick cirrus cloud and degraded even in light cirrus haze with reported visibilities of up to 50 miles.

Subsequent theoretical analysis resulted in the so-called "Hall criteria" [9] (see Fig. 1), which propose the existence of a minimum critical particle size and a minimum ice crystal concentration, both of which must be exceeded for any affect to occur. If particles of larger dimensions are present at higher concentrations, the achievable extend of laminar flow reduces with particle flux until a level is reached, where the boundary layer is entirely turbulent.

However, Davis et al. [5] pointed out that the findings illustrated in Figure 1 are limited to a Mach number of 0.75 flown at an altitude of 40,000 ft. Furthermore, the data is based on an elliptical approximation of the X-21 wing leading edge and the assumption that a cylinder with a length-to-diameter ration, *l/d*, of 2.5 is an adequate representative of most frequently occurring ice crystals. A further limitation was seen by Pfenninger [25] in the sweep angle, as an alteration of this would also change the particles' residence time within the boundary layer and the span-wise deflection of affected boundary layer velocity profiles.

There is however evidence from flight test results that a laminar boundary layer maintained from LFC technology is capable to tolerate the existence of ice crystals within the flown through surroundings if certain critical parameters are not exceeded. [8]

Overall, the effect of an ice crystal on an initially laminar boundary layer has been entirely attributed to its ability to produce turbulence within its wake. Assuming that any transitional behavior is bypassed due to the prevailing complexity of ice crystal shapes resulted for the above given flight envelop in the critical particle size shown in Figure 1.

Distribution A: Approved for public release; distribution is unlimited.

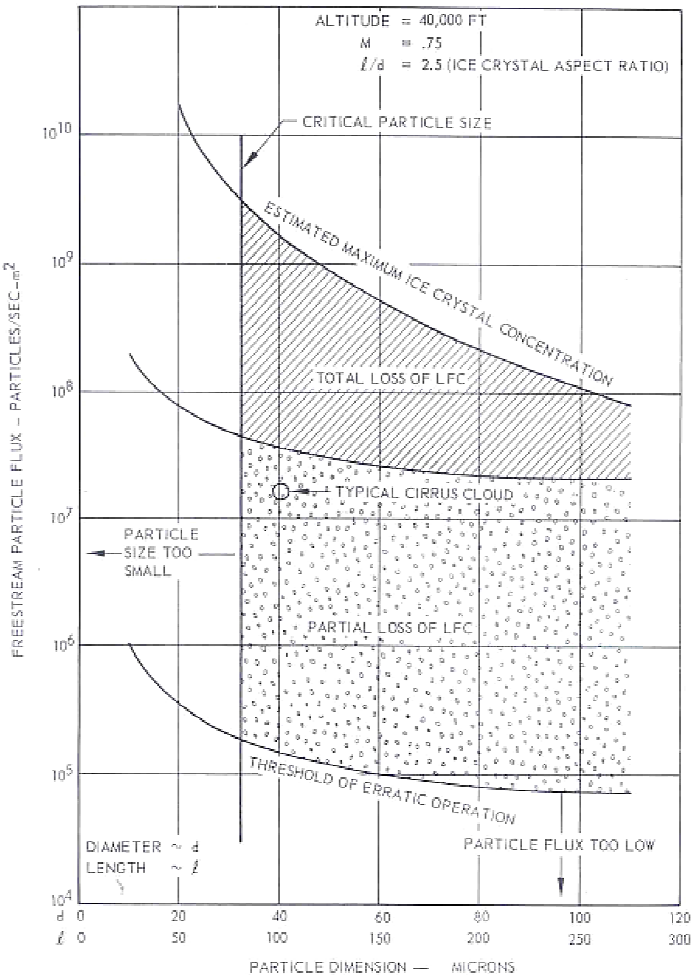

Figure 1 The „Hall Criteria", reproduced from Fowell & Antonatos [8]

The X-21 experiments concluded with full chord LFC not being applicable to production type aircraft, mainly due the fact that the required manufacturing tolerances were not achievable at that time.

The NASA LEFT Jetstar flight tests

In the mid 1980s, however, NASA decided to review the earlier made findings within their Leading Edge Flight Test (LEFT) program as part of the AirCraft Energy Efficiency (ACEE) program which had been launched in response to drastically increased fuel prices due to the oil crisis in 1973. The objectives were to determine (1) whether a slotted or a porous suction surface would be preferential, (2) to validate or not the findings of the Hall criteria, and (3) to identify how distinctive the effect of cirrus cloud on the performance of laminar flow technology would be along commercially flown routes.

Distribution A: Approved for public release; distribution is unlimited.

With regard to the Hall criteria [9], principal agreement could be achieved (see Fig. 2) in terms of the prevailing ice crystal concentrations; however, the employed Knollenberg probe was incapable of accurately identifying particles smaller than 60 µm at the speeds flown. Thus, the critical minimum ice crystal size could neither be confirmed nor abolished; in fact, a corresponding experimental verification has not been adduced until today.

Both, the X-21 and the LEFT Jetstar flight tests have described the detrimental effect of encountering cirrus cloud on the LFC performance as a reversible phenomenon, as the anticipated benefits immediately re-established after leaving a cloud in each case [5 ,9].

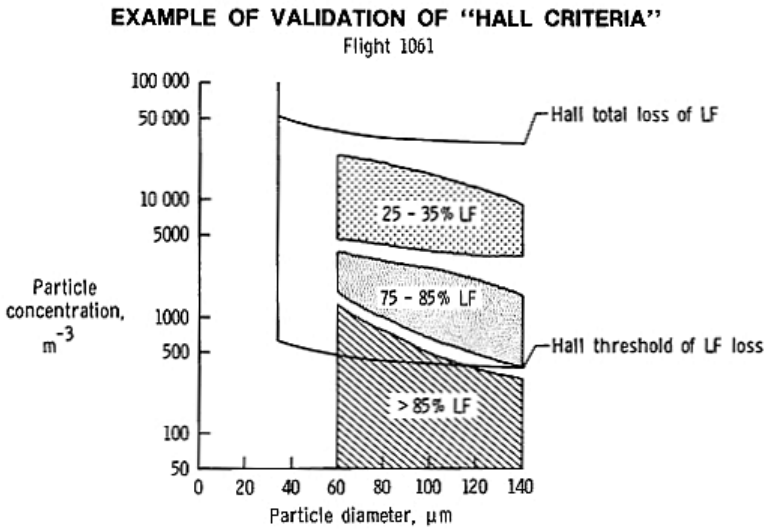

Figure 2 Comparison of results from the NASA LEFT program to the „Hall Criteria", reproduced from Davis et al. [6]

Knowing that the effect exists inevitably led to the question of how pronounced it is along typical commercial airliner routes. The required information could be obtained from the Simulated Airline Service (SAS) phase, during which the aircraft was flown in typical commercial environments out of three hubs within the United States (US), covering all seasons and a wide range of weather conditions. It should be noted that during the SAS no special maintenance in addition to normally applied standard procedures has been applied to the LFC systems without observing any major malfunction.

An overall average of 6 % per flight has been obtained, leading to the conclusion that the effect of ice crystals as occurring in cirrus cloud would not have a major effect on the feasibility of LFC applications [21].

Distribution A: Approved for public release; distribution is unlimited.

Analysis of GASP data

These findings were in good agreement to those from the analyses of more than 88,000 cloud encounter samples that have been recorded aboard four Boeing 747 aircraft in routine commercial airline service between 1975 and 1979 [13]. The data was available from the Global Atmospheric Sampling Program (GASP), which had monitored a wide range of environmental data along world-wide routes. [13]

However, it must not be overlooked that Jasperson et al. [14] concluded with seasonal and regional changes and thus with strong variability in the likelihood to encounter clouds from route to route. A corresponding example is illustrated in Figure 3 for a particular route.

Furthermore, it should be noted, that even though the majority of the flights could be shown to encounter clouds for less than the average, there occurred cases in both programs where on-route cloudiness was as severe as 50% [13, 21].

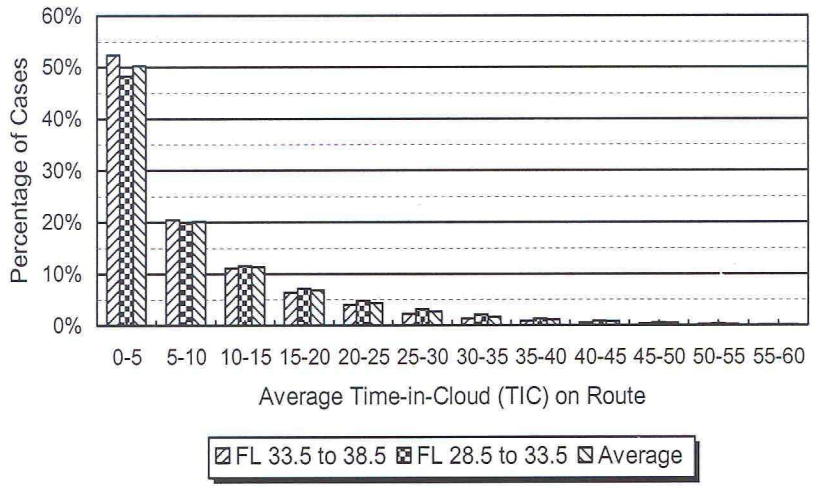

Figure 3 Typical GASP data for the US East Coast/NW Europe route, reproduced from Young & Fielding [41]

Impact on Flight Planning

In order to comply with stringent airworthiness requirements, always the worst possible case must be taken into consideration for fuel planning. As pointed out by Young et al. [42] the large variability in the observed data makes it difficult to plan the fuel required for a specific mission. If the periods of the flight during which laminar flow would be lost were known in advance, then the optimum fuel quantity could be up-loaded before departure.

However, without such advance knowledge a conservative assumption of, for example, a loss of laminar flow for 50% of the flight time would have to be made. This results in a greater fuel load on

Distribution A: Approved for public release; distribution is unlimited.

takeoff for most missions. And, as a jet airplane's fuel flow during cruise is approximately proportional to its weight (an airliner consumes about 3% of its current weight per hour in fuel), more fuel is thus burned due to the increased fuel that is up-loaded.

To fully capitalize on the potential of this technology further information is needed on the impact of ice crystals on laminar flow and on the incidence of cirrus cloud on flight routes. Young et al. [42] propose that, once sufficient information were available, a cloud parameter could be included within the fuel planning of future aircraft equipped with laminar flow technology. This could be applied in a similar manner as the wind parameter is used today. The preceding discussion identifies the future need for a reliable en-route cloudiness prediction tool, as suggested by Young et al. [42], if such laminar flow airplanes are to be operated to their full potential.

Previous laboratory studies conducted in air

As a natural consequence of the observations made during the X-21 test flights and subsequent analytical considerations, the phenomena were also examined in the laboratory. For this purpose, Hall [10-11] investigated the effects of the wakes from fixed, but elevated, particles in a laminar pipe flow at length Reynolds numbers from 1×10^6 to 3×10^6, based on the stream-wise distance from the pipe entrance to the particle location.

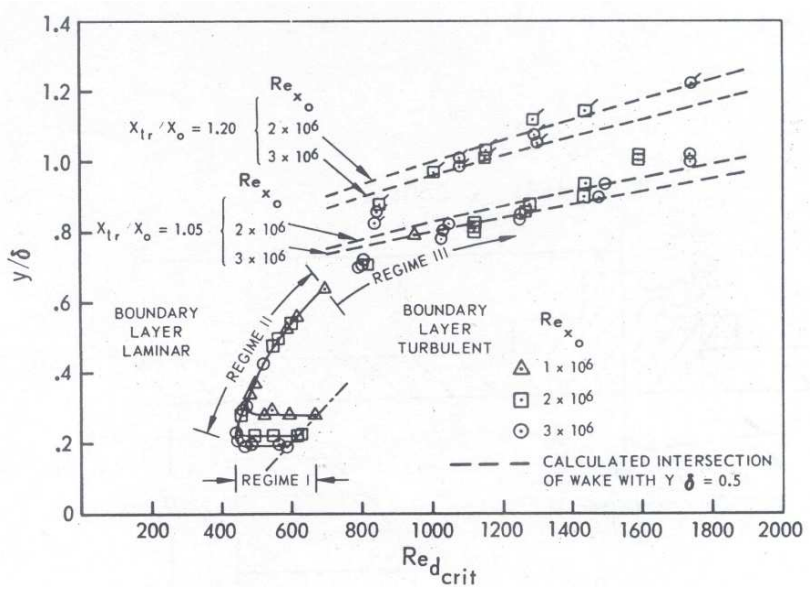

Figure 4 Variation of the critical Reynolds number with the ratio of transverse distance of the top of the sphere from the pipe wall, *y*, to boundary layer thickness, δ, reproduced from Hall [10]

Distribution A: Approved for public release; distribution is unlimited.

The pipe flow was undeveloped, thus providing for a stabilizing favorable pressure gradient due to the persisting boundary layer growth. It was found that spheres when exceeding a critical Reynolds number (derived from their diameter and the local undisturbed free stream velocity at the top of the particle) produced a steady turbulent wedge downstream of the element originating close to the object.

Being only slightly dependent on the length Reynolds number, this critical value was determined to vary between 585 and 665 for elements close to the surface. Since these numbers appeared to closely coincide with values where the onset of transition within the particle wake in a uniform flow field would be expected, Hall [10-11] attributed the effect entirely to the ability of the element's wake to spread turbulence into the laminar boundary layer. Thus, the "bypass" mode seems to be the driving mechanism in triggering the boundary layer transition rather than a disturbance of growing amplitude.

Regarding the influence of particle elevation from the surface, three regimes were distinguished (see Fig. 4). Regime I unveiled the surprising result that particles placed with their top at or below $y/\delta = 0.2$, having a smaller ratio of diameter to boundary layer thickness ratio, d/δ, than 0.2, affected the flow exactly like particles of the size d/δ equal to 0.2 as long as the gap between the surface and the particle did not exceed a critical value. In other words, within this region a small subcritical particle can produce the same effect as a considerably larger one that could be critical. [10-11]

In regime II, for $0.2 < y/\delta < 0.7$, the critical Reynolds number increases moderately with distance from the wall from a minimum of 450 to ~650, totally independent on the length Reynolds number within the investigated range.

Regime III, above y/δ of approximately 0.7, suddenly shows a very strong influence of the distance from the surface. Hall [10-11] attributed this influence to the ability of the spheres' wake to spread turbulence into a region below y/δ of approximately 0.4 to 0.5. This view is supported by observing a dependence of the stream-wise distance between the sphere and the origin of the wedge on particle elevation, as it will take the wake longer to diffuse into the aforementioned "trigger" region when it has to expand transversally from a further remote particle.

Hall's results compared well to data obtained by Mochizuki [23] during earlier wind tunnel experiments conducted on spheres attached to a flat plate. Mochizuki [23] proposed a dependence of the critical Reynolds number on the ratio of the sphere diameter, d, to the boundary layer thickness at the location of the sphere, δ. Extrapolation of the published information results in a minimum value of approximately 600 for $d/\delta << 1$. Unlike Hall's observations the turbulent wedge initiated not before some distance downstream of the element. This discrepancy was later be ruled out by Vincent [38], who investigated both surface attached and elevated spherical particles, and found that the wedge behind the former developed more gradually than past the latter case at matched conditions.

Distribution A: Approved for public release; distribution is unlimited.

Oceanic Applications

Unlike in air, most particles in water are nearly neutrally buoyant. Furthermore, the prevailing speeds are considerably lower. Nevertheless, the much greater dynamic viscosity of water (when compared to that of air) produces particle Reynolds numbers that are of similar orders of magnitude.

Since the particulate background level of oceans has been determined as generally being of too large diameters, drag reduction technology based on maintaining extended laminar flow regions does not seem to be feasible for oceanic applications. Nevertheless, the studies described below provide for some interesting insight that might be of important relevance when anticipating a study on the effect of free stream particulate on a laminar boundary layer.

Related research work carried out in water

Observations of laminar flow control performance degradation have been made during efforts to reduce the drag on marine bodies by thermal surface heating. Barker & Gile [2] have found discrepancies between their maximum achievable transition Reynolds number of 47×10^6 and the theoretically predicted value of 200×10^6 in a heated pipe flow experiment – a fact which they attributed to naturally occurring particulates contained in the water they used as the flow medium.

This effect could be substantiated by Lauchle & Gurney [16] during their experiments about a large heated ellipsoid in a water channel, where filtering the water for all particles larger than 5 µm considerably improved the performance.

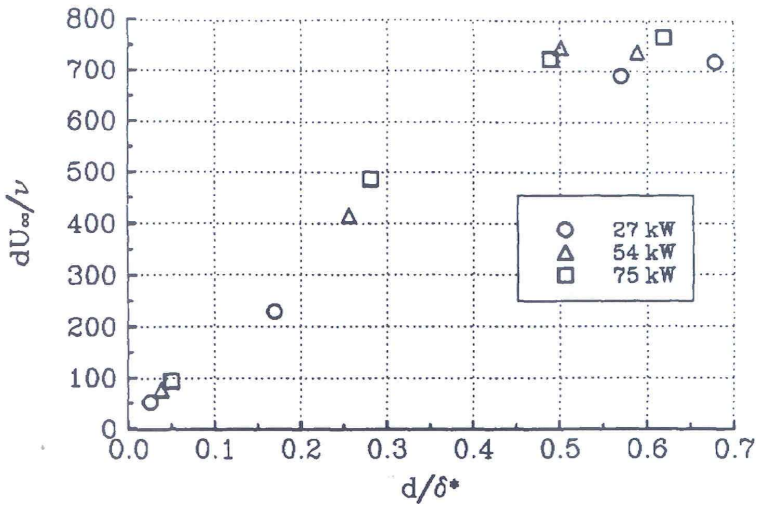

Figure 5 Estimated critical particle conditions on a heated laminar flow control body at three heating conditions, reproduced from Lauchle et al. [17]

Distribution A: Approved for public release; distribution is unlimited.

Unlike all other studies, these experiments (the focus of which had been set on the effect of the free stream particulate on the maximum achievable transition length Reynolds number at several heating levels) could not reveal the existence of a minimum critical particle size. It was found that all particle sizes considered detrimentally affect the maximum achievable transition length Reynolds number, this effect being greater, however, for larger particles (Fig. 5). For spheres with a diameter smaller than half the boundary layer thickness, there seems to exist a quite linear relationship of critical Reynolds numbers on particle size up to a certain point, from where on a constant number of 700 is proposed, which again compares well to observations made by other researchers [17].

In a further investigation it was anticipated whether or not the pure presence of the particles could cause the laminar flow to breakdown. The particles were introduced from a dye injection tube at the nose of the inlet. Surprisingly none of the particles, no matter what size, were found to have any influence on the laminar boundary layer supporting the hypothesis that there must be a sufficiently high slip velocity between the particle and the undisturbed flow for the above-described effects to occur [18].

A more controlled investigation in a similar experiment upon a smaller heated ellipsoid has been carried out by Ladd & Hendricks [15], where four different particle sizes were seeded into the free stream selectively. For the two lower particle sizes (12.5 µm and 38.9 µm), no measurable effect on transition could be identified when compared to the "clean" viz. filtered water case. Injected plant pollen of approximately 85.5 µm, however, caused the transition delaying effect of the heating to be totally lost above a length Reynolds number of 4.5×10^6 about the ellipsoid. Unexpectedly, this effect was reduced with the larger 132.2 µm polystyrene divinylbenzene (DVB) particles, leading to a further study of particle concentration variations. Within this study, it could be clearly demonstrated that the particle concentration has a strong influence on the transition location at the impacted body. Interesting is the plateau which formed at the higher concentration levels of the 85.5 µm particles, possibly indicating a limit at which a further increased particle number density would not cause a further increased deterioration for a particular particle size.

Petrie et al. [24] re-investigated the matter in a two-fold way by carrying out experiments on both fixed and freely suspended particles. While the observations made by previous researchers could be generally substantiated for the fixed sphere case, the mechanisms leading to transition due to freely suspended particles was described as being substantially different. Most importantly, it was noted that neither a horseshoe vortex nor hairpin-shaped vortices have been observed in the freely convected particle case. This observation led Petrie et al. [24] to the statement that "…convecting particle wakes have little, if any, affect on turbulent spot generation…", which is in clear contradiction to Hall's assumptions. [9] The rapidly developing spot, occurring as similar to the fixed case at Reynolds numbers exceeding 700, was attributed to disturbances brought about by the impacting particle to the

Distribution A: Approved for public release; distribution is unlimited.

laminar boundary layer near or below $y/\delta \sim 0.2$. Furthermore, in some of the convecting particle experiments the flow visualizations illustrated span-wise fluctuations ahead of the generated turbulent spots. This could not be observed when investigating particles at a fixed position. However, due to the short time scale between particle impact and spot emergence, a nonlinear growth of these disturbances has been suggested, thus not questioning the bypass-mode as being the triggering mechanism.

Aerodynamics of Blunt Bodies

The aerodynamics of blunt bodies has been the matter of interest for many studies. Of special interest in this case is the cylindrical shape, since this approximation was believed by Hall [9] to be valid for an ice crystal, and the spherical shape to which much of the analytical work in particle dynamics relates. It should be kept in mind, however, that in reality the design of ice crystals is rather irregular. The wakes forming behind cylinders and spheres will now be reviewed, and thereafter arbitrary shapes will be considered.

Cylinders: Roshko [27] provides a detailed study of the wake development downstream of cylinders, which was based on wind tunnel experiments. Three different regimes could be distinguished: the stable range for Reynolds numbers (*Re*) of 40 to 150 based on the cylinder diameter, a transitional range for a *Re* between 150 and 300, and the irregular range for $Re > 300$.

Within the stable range, the familiar pattern of the so-called Karman vortex street forms, a pair of counter-rotating vortices alternately developing from the upper and the lower separation point of the cylinder. The wake will remain entirely laminar. On the other end, in the irregular range, turbulence is produced right from where the vortices are generated. The transitional regime is characterized by laminar vortices separating from the cylinder's surface, which breakdown to a fully turbulent wake approximately 40 to 50 diameters downstream of the object.

However, Hall [9] pointed out that short cylinders ($L/d <= 5$) will suffer from vortices developing from their flat edges and should be considered as three-dimensional objects, which bypass the transition regime. This view is supported by the rather sharp edges that are found in real ice crystals (commonly described as hexagonal columns). Thus, the critical Reynolds number ($Re_{,crit}$) above which turbulence in the wake of a cylindrical particle can be produced, is assumed to be in the order of 150.

The frequency, at which this phenomenon occurs, has been shown to be represented by the Strouhal number, *St*, with excellent agreement [27]. Thus, the graph of *St* versus *Re* provides the time frame within which a particle can produce a turbulent disturbance. Knowing the residence time of a particle within the boundary layer will help to determine whether or not a disturbance of the laminar flow is likely to result in each case.

Distribution A: Approved for public release; distribution is unlimited.

Spheres: Due to its three-dimensional character, the wake behind a sphere is a little more complex and has been extensively studied in a uniform flow by Sakamoto and Haniu [28], whose results can be summarized as follows:

While increasing the Reynolds number, starting from very low values, the formation of a separated vortex ring at the rear of the sphere is observed as well as a long straight streak line along an axis through the centre of the sphere parallel to the free stream, which begins showing a periodic pulsating motion above Reynolds numbers of 130. This wave-like wake develops into so-called hairpin shaped vortices, which are periodically shed with equal strength and frequency as soon as a Reynolds number of 300 is exceeded. This represents the onset of the regular range.

At a Reynolds number of 420, the shedding direction starts to oscillate intermittently from left to right until no further signs of regularity in the vortex shedding are apparent at Reynolds numbers above 480. Within this region, termed the irregular range and ranging up to Reynolds numbers of 650, the shedding pattern of vortices is always in the irregular mode. Furthermore, the shedding direction is described as rotating slowly and irregularly about an axis through the sphere's centre along the velocity vectors of the undisturbed flow.

At further increased Reynolds numbers, some regularity can be observed again in the vortex shedding pattern being linked to the onset of pulsation of the cylindrical vortex ring. The vortex tubes periodically shed in this way diffuse near the sphere without retaining their cylindrical shape. Additionally, the large scale hairpin-shaped vortices transition from a laminar to a turbulent state.

Above Reynolds numbers of 800 the wake is described as being fully turbulent. Besides the large vortices, which are obscured in their form now, the smaller scaled vortices shed from the cylindrical vortex ring partially cease to diffuse now and interact heavily with their surroundings, while being transported downstream. This is connected with a bifurcation of the vortex shedding frequency into a high-frequency mode associated with the smaller vortices and a low-frequency mode, with which the larger vortices are shed.

Two further regions have been identified at still larger Reynolds numbers. However, due to the expected size of the particles under consideration, they are of little relevance for this study.

Later investigations have been carried out in a uniform shear flow and revealed that the critical Reynolds number is increased under this condition. Furthermore, it was found that the vortices always detach at the high velocity side and that the Strouhal number increases with the local shear parameter, K, which is defined as the local transverse velocity gradient, G, non-dimensionalized by the free stream velocity, U_∞, and the sphere diameter, d. The regular region starts to develop at slightly lower Reynolds numbers compared to the uniform flow case and the shedding frequency is determined to also increase with K [29].

Distribution A: Approved for public release; distribution is unlimited.

Arbitrary Shapes: There is only sparse information about the wake characteristics of irregularly shaped elements. Investigations of discs and flat plates normal to the free stream represent worst case scenarios and are of little interest for this study. However, some quantitative information can be found in Hall [11], where it has been observed that replicas of ice particles that were collected in flight, termed as "quasi-spherical elements", where found to yield similar results to those of a sphere. Depending on the grade and the orientation of the irregularities the critical Reynolds number was found to lie between 75 to 100 % of the sphere's value.

Explorations concerning a double-sided cone of length-to-diameter ratio of 2.5 resulted in answers similar to that of a cylinder of the same ratio, the critical Reynolds number being a little larger for the former. It is interesting is to note that the measured data did not change significantly for angular deviations of +/-30° about the anticipated orientation of the particular element (with its axis normal to the approaching flow) for both cases. Thus, possible oscillations about their axis, which are likely to occur while travelling within certain Stokes number regimes as described in Loth [19], are not likely to have a major effect. Surprisingly, despite the low length-to-diameter ratio, the measurements on the cylinder compared favorably to earlier experimental results obtained for purely two-dimensional tripping elements [27].

The above information led Hall to revise his originally proposed minimum effective diameter for a Mach number of 0.75 at 40,000ft from 32 μm (see Figure 1) to a three-fold value of about 90 μm. Similarly, he increased the corresponding value for the same Mach number at 25,000 ft from 17 μm to 50 μm. [11]

Distribution A: Approved for public release; distribution is unlimited.

Methods, Assumptions, and Procedures

Laboratory issues and the particles' view

In order to capture all mechanisms occurring in reality due to the above described combination of parameters by the conventional approach of positioning the model (object of interest) at a fixed location and forcing the fluid (air in this case) to flow over it (i.e. the common methodology for wind tunnels and water channels), would require the experiments to be run at very high speeds. This however, results (as in reality) in very thin boundary layers that can only be analyzed with great difficulty. Anticipating detailed investigations of the wake effect of an even smaller suspended particle on such a boundary layer is considered by the author to be impossible without extremely sophisticated measurement techniques of the latest state of the art. Furthermore, the recreation of a cirrus-cloud-like environment for extended periods of time is costly and would require a closed-loop wind tunnel, which will be subject to a degree of wear due to the particles repeatedly passing through the fan. Furthermore, it is likely to introduce additional health and safety concerns for the investigators.

Making use of a water channel instead, which can often overcome problems encountered with laboratory work involving gaseous flow, would not be adequate in this case, as no known matter is heavy enough (in comparison to water) to produce even comparable inertia forces. Therefore, the relative velocity component in the stream-wise direction (between the particle and the water) would diminish and thus not provide the desired results (Fig. 6).

An alternative approach that has been considered is to reduce the speed of the wind tunnel experiment, as this would achieve thicker boundary layers and simultaneously slow down the effective mechanisms. However, this method will automatically necessitate lighter particles; otherwise they won't be as easily transported by the carrier fluid as in the original case.

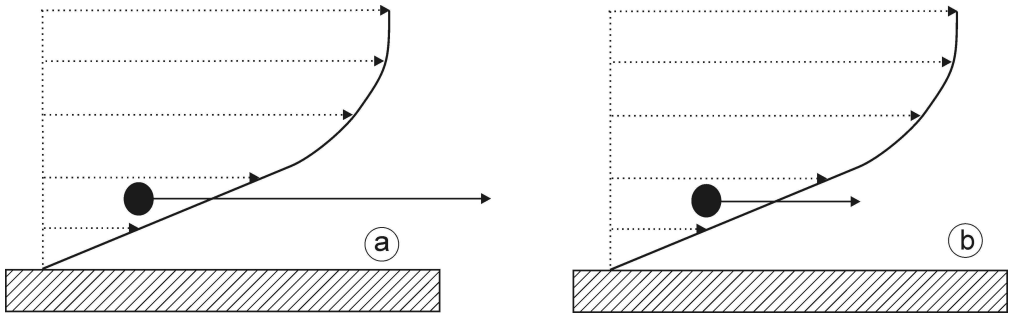

Figure 6 The adaption of the stream-wise velocity component due to alterations of the density ratio between the particle and the carrier fluid. Shown are the original case for a heavy particle (a) and a nearly neutrally buoyant particle (b).

Distribution A: Approved for public release; distribution is unlimited.

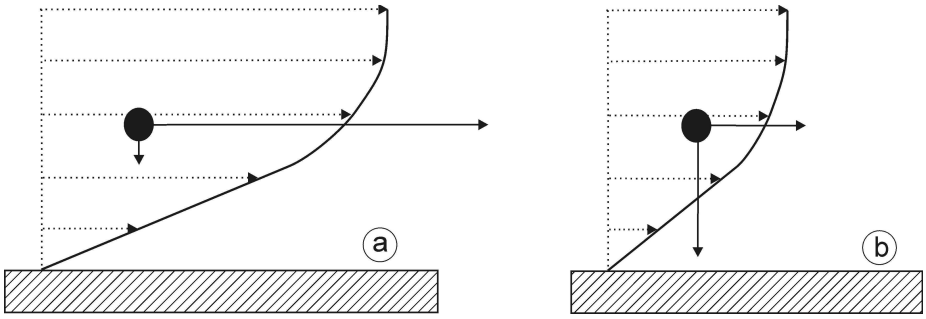

Figure 7 The changing ratio of the wall normal and stream-wise velocity components due to alterations of the free-stream speed. Shown are the velocity vector components of a particle at high (a) and at low free stream velocity (b).

This in turn would result in a progressively pronounced effect of the vertical velocity component in comparison to the stream-wise direction, which contradicts the initial assumption of the vertical velocity being negligible (Fig. 7). Furthermore, considerable disagreement can be expected when comparing trajectories.

On the other end, making use of lighter particles will also reduce their inertial forces. Together with the effect of a thicker boundary layer and a reduced speed at the boundary layer edge, the particles are progressively inclined to adapt to the velocity changes of the shear layer profile (Fig. 6). This will introduce errors very quickly: a particle size that could be critical in the real case is not likely to show an effect in the laboratory when adopting this procedure.

Also, attempts have been made to fix the particle at several heights within the boundary layer [10, 11]. This method has the great advantage of eliminating the vertical velocity component while enabling measurements to be taken within the effective non-uniform stream-wise velocity field. The particle investigated in this manner will always experience the largest relative velocity on its side farthest from the wall. However, as the particle, in reality, is moving with the free stream, the critical side should in fact be the one adjacent to the wall.

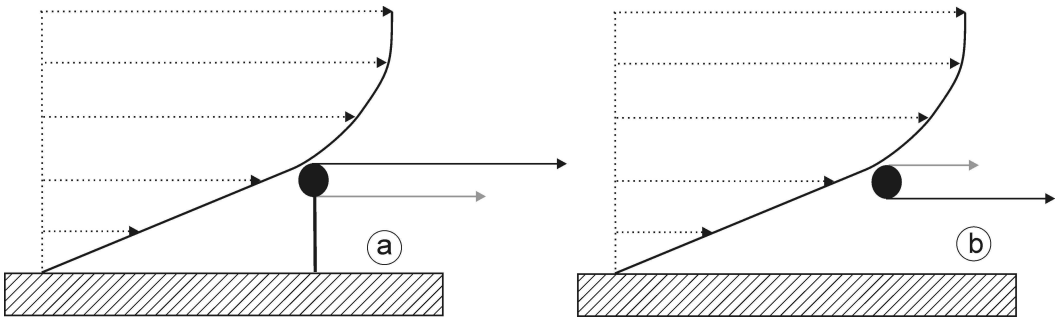

Figure 8 The stream-wise relative velocity magnitude experienced by a particle immersed in a boundary layer at each of its sides (top and bottom). Shown are the prevailing situations for a fixed (a) and a suspended particle (b). Note, that in the suspended case the particle will develop its wake in the opposite direction.

Distribution A: Approved for public release; distribution is unlimited.

As the velocity gradients are substantially larger in the boundary layer's near-surface regions, this procedure is likely to produce considerable disparity (Fig. 8). Additionally, for this method a critical particle will always be critical before entering the boundary layer, being in clear contradiction to the original case, in which the ice crystal's relative velocity tends to zero within the free stream.

Furthermore, it may be pointed out that in reality the stream-wise velocity vectors are generally of opposite orientation when compared to the conventional laboratory case (e.g. wind tunnel) (see Fig. 9). Whereas, this is of no consequence for standard aerodynamic investigations, it might be one cause for the observed differences in previous analyses of the particular case of a boundary layer affected by freely suspended particles.

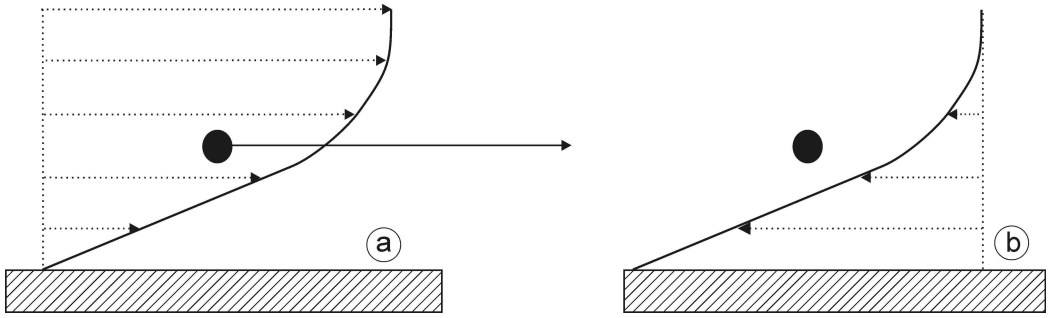

Figure 9 The differences in the orientation of the velocity vectors. Shown are the situations as occurring in a conventional laboratory experiment (a) and in reality (b).

An alternative experimental method

The great difficulties encountered while attempting to recreate conditions in the laboratory that are representative of the real occurrences, and the considerations discussed in the preceding sections have led to an alternative experimental approach. This involves reversing the commonly-employed approach of a wind tunnel in terms of moving a surface within a test section (e.g. one of its side walls) which is filled with a fluid that is at rest, at very low, or more precisely at "subcritical" speed. Such an approach would allow for positioning the particle at a fixed position, while at the same time processes could be slowed down, thus providing for relatively thick boundary layers. Additionally, important key features, as for instance the direction of the velocity vectors, the position of the critical condition, and the insignificance of the particles' wall normal velocity component, are preserved.

This method is hoped to shed further light onto the mechanisms occurring when investigating the effect of particles that are in equilibrium or near equilibrium to a carrier fluid before entering a shear layer. It is believed to be a suitable approach for investigating the wake development of a particle immersed into a wall-bounded non-uniform shear flow, thus being capable of identifying the needed critical particle parameters.

Distribution A: Approved for public release; distribution is unlimited.

According to theory (First Stokes Problem), however, the boundary layer over an infinitely large flat plate set suddenly into motion has been proposed to grow as [30]:

$$\delta = 3.6\sqrt{\nu t}\ . \qquad \text{Eq. 1}$$

In other words, the boundary layer will steadily continue to thicken with time. Nevertheless, it is characteristic for a root function to have its steepest gradients near zero. Thus, by assuming a constant dynamic viscosity, the rate of increase in boundary layer thickness will reduce with duration and may be negligible after some run up time for a certain period of time, within which meaningful measurements could be taken.

Furthermore, Eq. 1 describes a mathematical model based on boundary conditions that, according to everyday's experience, do not necessarily apply to practical applications. In other words, when imagining a plate attached to a flying aircraft, the initial condition at its leading edge would be constantly reset to zero, since fresh air parcels (being "quasi-at-rest") are continuously approached. The anticipated method aims at achieving similar conditions by forcing a constant rebuilt of the prevailing boundary layers due to the wind-tunnel-like configuration.

Preliminary Computational Fluid Dynamics analysis

In order to obtain an initial proof of concept for the anticipated approach a preliminary Computational Fluid Dynamics study has been made. Within this, the most critical features of the planned setup were attempted to be reproduced, namely the rotational drum bounding the inner side of a semicircular test section.

The required computational mesh was generated by using the meshing tool GAMBIT and consists of 40,000 quadrilateral cells, of which 200 are attached to the rotational drum. The resolution of the mesh is greater in regions where greater computational accuracy is needed, i.e. close to the drum. Cell face areas range from 0.0005 m^2 to 0.0057 m^2.

The simulation was run using the FLUENT software package, into which the generated mesh has been loaded to a double precision solver. Much consideration was given to defining a suitable setting of boundary conditions (BC), which were set to either in/outflow or pressure in/outlet. The velocity inlet condition, frequently used for conventional wind tunnel investigations was not deemed to be suitable, as this restricted the free inflow due to a fix definition of the inflow velocity at each computational step over the entire inlet. The drum was defined as a moving wall and set to rotate at a speed of 4 m/s (25 rad/s).

Due to the steady build-up of the boundary layer (as expected from theory) the decision was made to run the simulation with an unsteady solver. Surprisingly, the initially rapid boundary layer

Distribution A: Approved for public release; distribution is unlimited.

growth seemed to stop after only a few seconds of simulated time and only minor changes in the boundary layer thickness were apparent thereafter (see Figure 10). This was further substantiated by the characteristics of the monitored error functions, showing that the solutions for the computation of subsequent time intervals could (after some run time) be found within the first step of each subsequent interval, thus representing a quasi steady behavior.

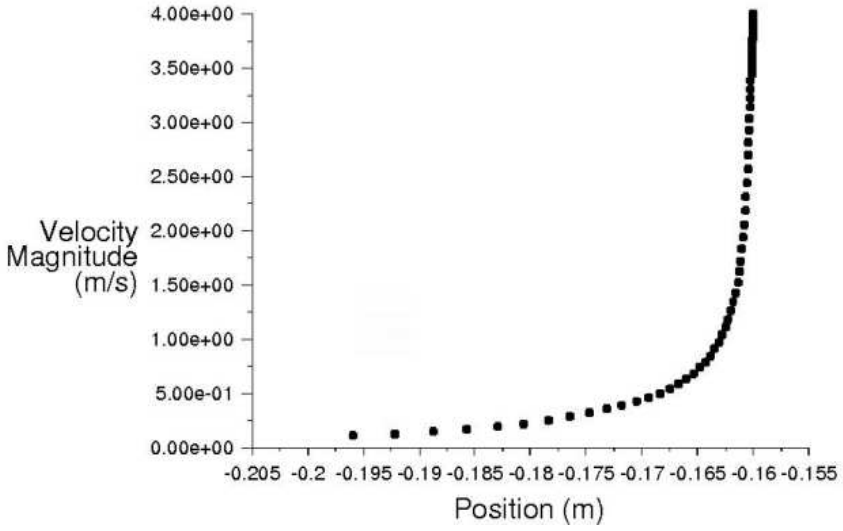

Figure 10 Quasi-steady boundary layer velocity profile, which was established for an unsteady simulation after a period of approximately 8s (Note, this is a turbulent solution).

It should be noted that the model was run initially as a turbulent simulation (based on a standard k-ε-turbulence model). After converging, the solution has been used as the initial condition for the laminar solver. This procedure has been chosen based on experience, since convergent laminar solutions are very time-consuming and difficult to obtain. Proceeding as described above however considerably reduced computational expenses and provided the desired solutions in a timely manner.

Figure 11 shows the obtained "steady" laminar solution of the boundary layer at a position half way between in- and outlet of the test section. As can be seen, the resulting boundary layer thickness is somewhat larger than, for example, a Blasius solution, even though the constant cross sectional area throughout the test section length, should provide for a near zero pressure gradient flow. This can probably be attributed to the curvature of the test section resulting in some inertial forces.

A 3D simulation was also run, since it is generally believed that they are more accurate; however, the solution did not achieve the quasi-steady characteristic described above for the 2D case. Nevertheless, convergence could be achieved for each time step after a few iterations. Again, after a few seconds of simulated time the changes in boundary layer thickness were too small to distinguish the solutions of different time steps.

Distribution A: Approved for public release; distribution is unlimited.

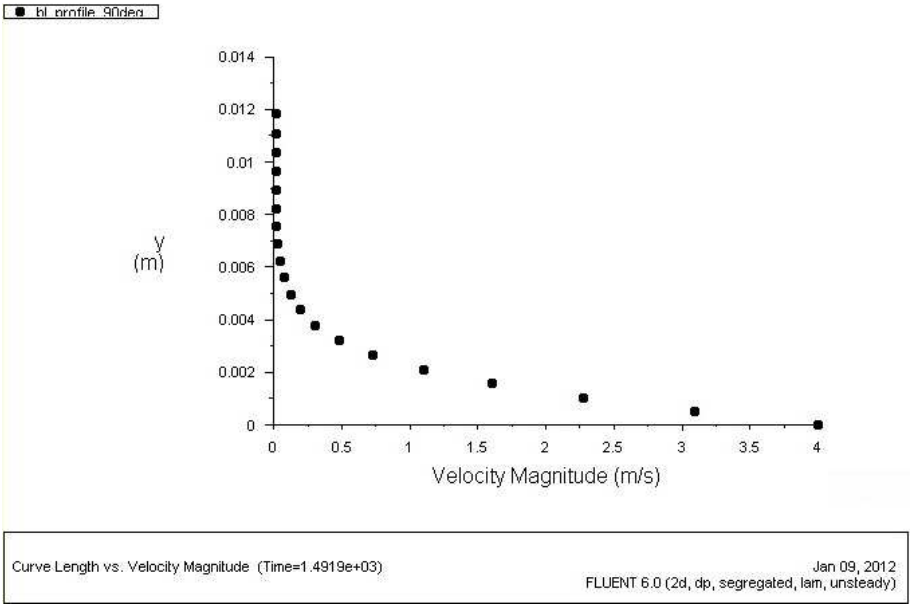

Figure 11 Laminar boundary layer velocity profile determined mid-way between in- and outlet (two-dimensional laminar solution)

In summary, the results obtained from the CFD analyses support the initial assumptions on the feasibility of the anticipated approach. However, it is generally accepted, that computations are meaningless without being able to benchmark results to a practical application. Thus, the logical consequence was the attempt to build and test a novel experimental device.

Design and Manufacture of the Test Facility

The test facility has been designed around a circular drum, which can be rotated in order to provide for the required moving surface. At the same time, it replaces one of the test section side walls. Figure 12 shows a principle sketch of the anticipated facility. This approach has been chosen in preference over the more commonly found method of moving a straight wall, as it considerably reduces the complexity of the setup. Furthermore, it overcomes a number of issues that are usually connected to a driven belt configuration, like for instance smoothness, rigidness, waviness and durability, making the choice of the right material a very difficult task.

The drum has been made of a 208 mm long section of a steel pipe to which a side wall has been welded on either side, resulting in a closed-up compartment. Along the centerline a 20 mm rod has been fitted, providing for the axle to which the bearings and a v-belt pulley to drive the drum can be attached.

Distribution A: Approved for public release; distribution is unlimited.

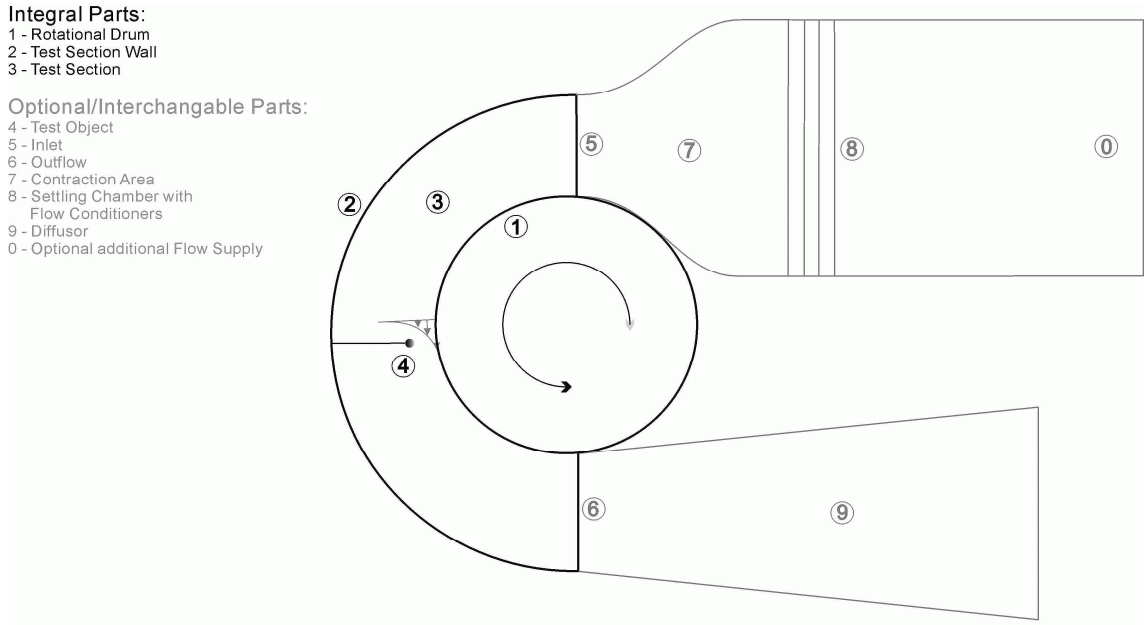

Figure 12 Principle example sketch of the test facility (side view)

From one side a 5 mm hole has been blind-drilled into the rod along its axis for about half of its length. At the end of this hole, another one has been fitted perpendicular to the former, going all the way through the rod. This provides for access to the inside of the compartment, which can thus be filled with smoke during the experiment if required. Subsequent to the complete assembly of the drum, its outer surface has been machined to the desired dimension to achieve the highest possible degree in concentricity. The resultant diameter amounts to 322 mm providing for a run length of approximately 1 m per rotation.

The test section is bent around the rotational drum with a squared cross-sectional area of 210 mm side length. Since it is entirely made of plexy glass, it provides for great visible access from all sides. The two 10 mm thick straight side walls are centered on the drum's axle and curved on the other side with a 361 mm diameter. Along the curved ends, a 3 mm thin plexy glass sheet has been attached providing for the outer test section wall.

For reasons stated above, it has been decided to design the reminder of the facility in accordance to a conventional wind tunnel approach, involving a contraction area and a diffuser, as well as a settling chamber to which a potentially required additional flow supply can be attached. The only non-standard component is an 1800 W electric motor, which drives the drum over a v-belt configuration.

The general purpose of the contraction is to reduce the variations of the mean and fluctuating velocity variations, and to increase the flow speed delivered from a flow supply. It is defined by its length, l, the contraction ratio, c and its contour. Regarding the latter, it is desirable to have a wall profile with zero second derivatives at both in- and outlet. Furthermore, a widely accepted view is that

Distribution A: Approved for public release; distribution is unlimited.

the most favorable combination of flow uniformity, thin boundary layers and negligible losses can be achieved when providing for inlet and outlet profile radii that are roughly proportional to the area. The fifth-order polynomial proposed by Bell & Metha [3] has been successfully applied in many low speed tunnels. However, while providing for the desired derivatives, the second condition on the radii is not fulfilled (see Eq.2). This inspired Brassard & Ferchichi [4] to work out several modifications of the above mentioned polynomial. Based on the results of a numerical evaluation of this matter [7], the subsequent profile has been chosen for the 500 mm long contraction of this test facility, using *f(ξ) = x/l in Eq. 4*:

$$h = [-10\xi^3 + 15\xi^4 - 6\xi^5]\left(1 - \frac{H_o}{H_i}\right) + 1 \qquad \text{Eq. 2}$$

$$\eta = [10\xi^3 - 15\xi^4 + 6\xi^5] \qquad \text{Eq. 3}$$

$$h = \left\{-\eta\left[1 - \left(\frac{H_o}{H_i}\right)^{1/f(\xi)}\right] + 1\right\}^{f(\xi)} \qquad \text{Eq. 4}$$

Where, $h = y/H_i$ is the contraction height, y, normalized by the contraction inlet height, H_i; H_o is the contraction outlet height, $\xi = x/l$, *and* η simply replaces the core polynomial of the original equation (Eq. 2) for ease of use in Equation 4.

A diffuser is defined by its area ratio, A_e/A_i, and an equivalent cone angle, θ [26]. This angle is the overall angle enclosed by a frustum having the same cross sectional area at both the inlet and the outlet openings. Separation in the diffuser can cause velocity oscillations in the test section (often called surging) and thus needs to be avoided. At the same time, it is desirable in most cases to recover as much pressure as possible. A workable compromise, frequently proposed, places the cone angle at about 5° [22]. However, considering both, a possibly still laminar boundary layer at the exit of the test section and the expected greater than normal boundary layer thickness, the decision was made for a slightly smaller cone angle of 4°. This view is further supported by the fact that due to the open-circuit configuration of the tunnel, pressure recovery is not a decisive design criterion for this project. The resultant diffuser has an area ratio of 2 over its length of 1500 mm.

The settling chamber commonly holds both, screens and honeycombs to condition and straighten the flow delivered from the blower before it enters the test section via the contraction. Whereas the former reduces the longitudinal velocity variations of the flow, the latter removes the lateral ones as well as the swirl.

Distribution A: Approved for public release; distribution is unlimited.

Figure 13 The particle wake investigation test facility (University of Limerick)

In order to reduce manufacturing cost, it was decided to base as many components as possible on standard off-the-shelf materials. A further objective was to obtain a high degree of flexibility. This was achieved by a frame construction based on box steel, which allows for a time-efficient attachment of potentially required additional equipment. Furthermore, the facility allows for interchanging all in- and outflow components, which may be desirable in order to obtain a specific flow condition within the test section. Since the experiments are likely to require a quiescent environment, the decision was made for a mobile construction that can be moved effortlessly to a suitable area. In Figure 13, the completed particle wake investigation test facility is shown.

Testing the Equipment, and Proof of Concept

As soon as the test facility was assembled, a quick preliminary test has been done by traversing a standard pitot tube in the wall normal direction of the rotational drum at a single stream-wise position near the centerline of the test section. Figure 14 shows the obtained velocity profile in non-dimensionalized parameters based on an estimated shear layer thickness of 100 mm. The measurements were taken at a location about 300 mm downstream of the test section inlet for a drum rotation of 300 rpm, thus approximately 5 m/s. This provided for a length Reynolds number, *Re*, of 107,000. As is apparent from the illustration, a certain amount of stream-wise flow velocity could be detected throughout the entire height of the test section, which is unlike the results proposed by the

Distribution A: Approved for public release; distribution is unlimited.

CFD investigation. Nevertheless, a boundary layer like flow profile develops within a few seconds and measuring the same values at the same wall normal distance repeatedly, points out that a stable equilibrium can be achieved for the flow. This represents an initial fulfillment of the anticipated target and thus provides for a proof of concept.

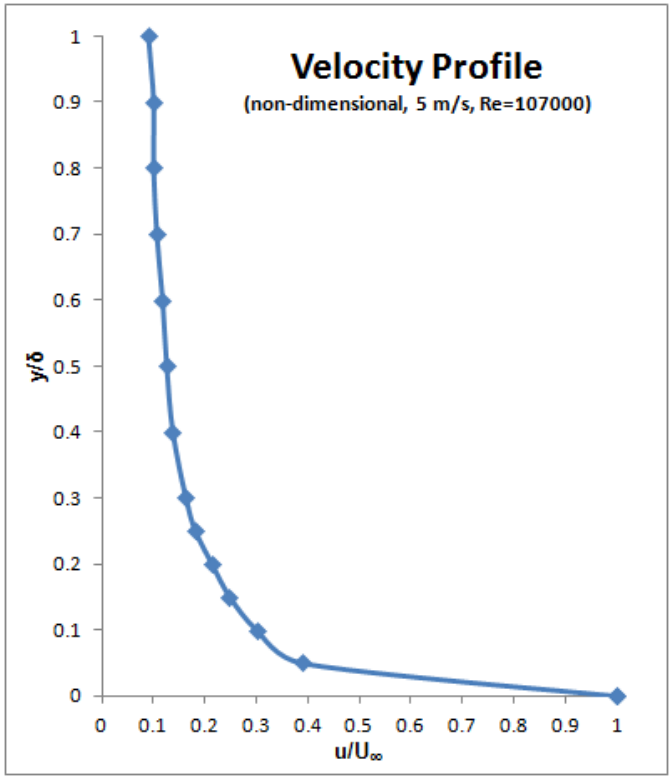

Figure 14 First boundary layer velocity profile measurements providing for the required proof of concept.

It must be noted, however, that at the time these initial measurements were taken, the rig was subjected to a serious vibration issue, which has meanwhile been overcome by statically balancing the equipment. Furthermore, the drum's surface was covered by a thin layer of silicon oil, which had been applied during manufacture as a rust prevention measure. Therefore, it is not clear whether or not the air particles adjacent to the surface actually achieved the anticipated speed of 5 m/s. It could therefore be speculated that more rigidly enforcing the no-slip condition could result in even more air being dragged along with the rotating surface, thus leading to an even higher "background" velocity within the test section.

Distribution A: Approved for public release; distribution is unlimited.

Preliminary Results

The shape of the velocity profile shown in Figure 14 appears somewhat fuller than the result obtained from the CFD study (see Figure 11). Furthermore, the thickness of the developing shear layer raised concerns that the flow could have been turbulent and emphasized the requirement to appropriately characterize the flow. In order to obtain some greater insight, smoke flow visualization was conducted to investigate the flow. Furthermore, it has been decided to reduce the speed of the rotational drum to 175 rpm, which is equivalent to 2.95 m/s. The smoke has been introduced near the test section inlet at the upper side of the contraction. This is close to the position where the shear layer over the drum begins to develop. The illustration on the left hand side of Figure 15 clearly shows turbulent structures along what is believed to be the edge of the shear layer.

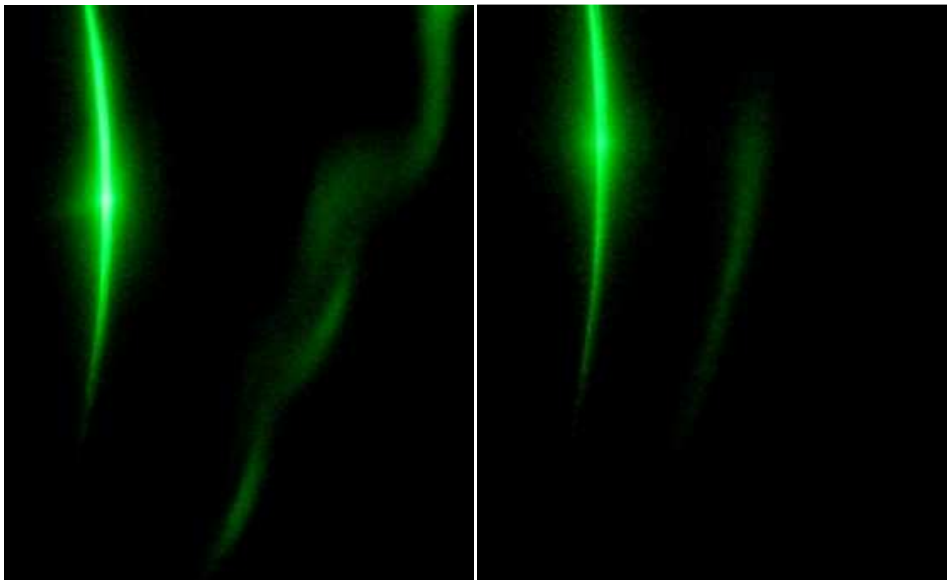

Figure 15 Example illustrations of the smoke flow visualization showing turbulent structures on the left hand side, which have disappeared after improving the inflow conditions on the right hand side.

This observation has led to a modification of the inflow conditions by adjusting the contraction outlet in such a way that a small gap rather than a step was present. This gap was covered by a 20 µm thin PTE foil that smoothly attaches to both the contraction contour and the surface of the rotational drum. The photography on right hand side of Figure 15 has been taken subsequent to this modification making apparent the achieved improvement.

Both situations have also been investigated by traversing a total pressure head through the shear layer in the wall-normal direction. The static pressure reference was taken from a flush-mounted inlay at the test section sidewall, in order to eliminate the effect of being also partially subjected to dynamic pressure when using a straight standard pitot in a rotating flow. The obtained boundary layer traverses

Distribution A: Approved for public release; distribution is unlimited.

are shown in Fig. 16, together with a parabolic approximation for the velocity profile a flat plate laminar boundary layer as a reference (see Eq. 5). Also this data indicates that the modifications of the test section inlet have improved the flow quality, since the turbulent case shows the typical full profile near the surface. However, even though the "assumed laminar" case approaches the parabolic approximation, there are some differences. It is probable that this can be attributed to the great ambiguity involved in defining the boundary layer thickness. Nevertheless, more accurate measurements are required in order to reach confidence in this regard.

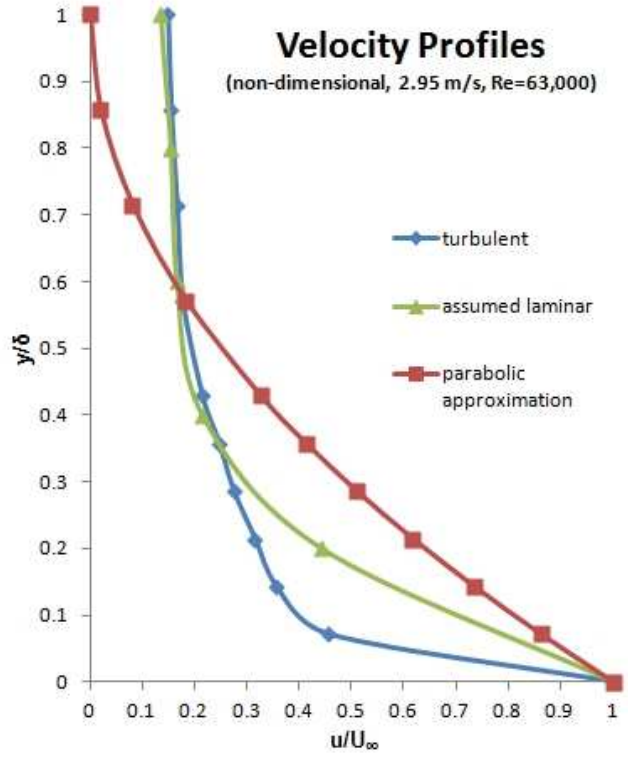

Figure 16 Examples of measured velocity profiles at rpm=175 (acc. to U_∞ = 2.95 m/s) in comparison to the elliptical approximation of a Blasius type solution.

The "background" flow, which has been described earlier, is again found to spanning the entire test section in all cases and seems to amount to about 15% of the rotational speed of the drum. However, since a stable equilibrium condition is established, this merely means that care must be taken for this phenomenon to remain sub-critical for a particle to be investigated. Within the regions adjacent to the drum's surface, the desired flow condition can be established with the test facility providing for a variety of opportunities for the anticipated particle wake studies.

Distribution A: Approved for public release; distribution is unlimited.

Preliminary Discussion

The assumptions that a particle can cause a laminar flow to breakdown as soon as a critical Reynolds number (based on its diameter and its velocity relative to the surrounding flow) is exceeded could be substantiated. Even though the agreement about the order of magnitude of such a critical value is generally good, the measured data show considerable scatter, ranging from 450 to approximately 1000, with values around 700 being the most frequent occurrence [10-11, 15-18, 23-24, 28-29, 38]. However, more previously made investigations of particles travelling through a boundary layer in air have found a value as small as 300 to be critical [31-33].

Besides, further influencing variables might play a role in the mechanisms for the phenomena to occur, amongst them the ratio of particle size to the local boundary layer thickness and the instantaneous distance from the surface. Hall [10-11] suggested, based on his measured results that a supercritical particle would only have an effect on the laminar boundary layer if its turbulent wake diffuses into boundary layer regions below y/δ of approximately 0.5.

Sakamoto & Haniu [29] have determined that in a uniform shear flow of sufficiently strong velocity gradient the familiar pattern of vortex shedding from alternating sides breaks down and the wake vortices will always originate from the high velocity side. This is of particular importance, when considering that the particle side closest to the surface (a wing for example) will generally be the critical one for the case of a cirrus cloud being approached by an aircraft.

As discussed in this document, the recreation of the desired in-flight phenomena in a laboratory is forbiddingly difficult due to the twofold mechanisms prevailing for a comparatively heavy particle travelling through a boundary layer at a typical aircraft cruise speed. The investigator was left with only two options when trying to obtain meaningful data from his experiments:

(1) a setup involving the real parameters in terms of wind tunnel speed as well as particle sizes and densities
(2) an attempt involving an alternative approach as for instance the one described within this document

Within this work, the second approach has been chosen by manufacturing an appropriate particle test facility, as this could result in obtaining greater insight into occurring mechanisms. First obtained results are encouraging.

Distribution A: Approved for public release; distribution is unlimited.

Experimental Work – Second Phase

Following major structural modifications of the test facility, which were completed during the proof-of-concept phase of this project, it was moved to the aerodynamics research laboratory of the University of Limerick, in order to obtain easier access to the required measurement equipment. Figure 17 shows the complete setup consisting of the test facility itself, the power supply, a manometer, a thin-sheet illuminating laser, a stepper motor controlled probe traverse system, a Hot Wire (HW) measurement acquisition system (TSI IFA 300), as well as two computers used to control the systems and for data storage.

Figure 17 The complete experimental setup of the new test facility in the aerodynamics research laboratory at the University of Limerick

Measurements with a purpose-built flattened Pitot tube

As determined during the proof-of-concept phase of this project, the free stream, which was initially anticipated to be entirely quiescent, performed with a uniform flow velocity in the order of 10% to 20% of the drum's rotational speed. However, it was found that blocking parts of the diffuser outlet, thus building up a slightly favourable pressure gradient, considerably reduced this effect (see Figures 18 and 19).

Additionally, as could be expected, this had a stabilizing effect on the developing boundary layer. A steady vortex, probably caused by a separation bubble occurring at about half way through the test section, could be moved downstream when applying some diffuser blockage (refer to the Smoke Flow Visualization section).

Distribution A: Approved for public release; distribution is unlimited.

The complete absence of previously published data from similar experiments posed a problem for this project in terms of benchmarking. Therefore, the decision has been made to compare the obtained results to the standard Blasius profile [30], which is a common procedure when dealing with zero pressure gradient flows, at least for flat plate studies. Since determining a valid x-value, which is required for the Blasius approach in order to calculate eta, η, did not seem to be a straightforward task for this experiment, the elliptical approximation as proposed by v. Karman (cf. White, 1998) [39] has been chosen, since it is only dependent on wall normal parameters:

$$\frac{u}{U} = 2\frac{y}{\delta} - \frac{y^2}{\delta^2} \qquad \text{Eq. 5}$$

where:
- u local stream-wise velocity
- U rotational speed of the drum
- y wall-normal distance
- δ local boundary thickness

Measurements taken with a purpose-built flattened miniature Pitot tube, which was attached to a stepper motor controlled traverse system enabled for more accurate readings to be taken and this provided for a surprisingly close match when compared to v. Karman's theory [39] (see Figure 18).

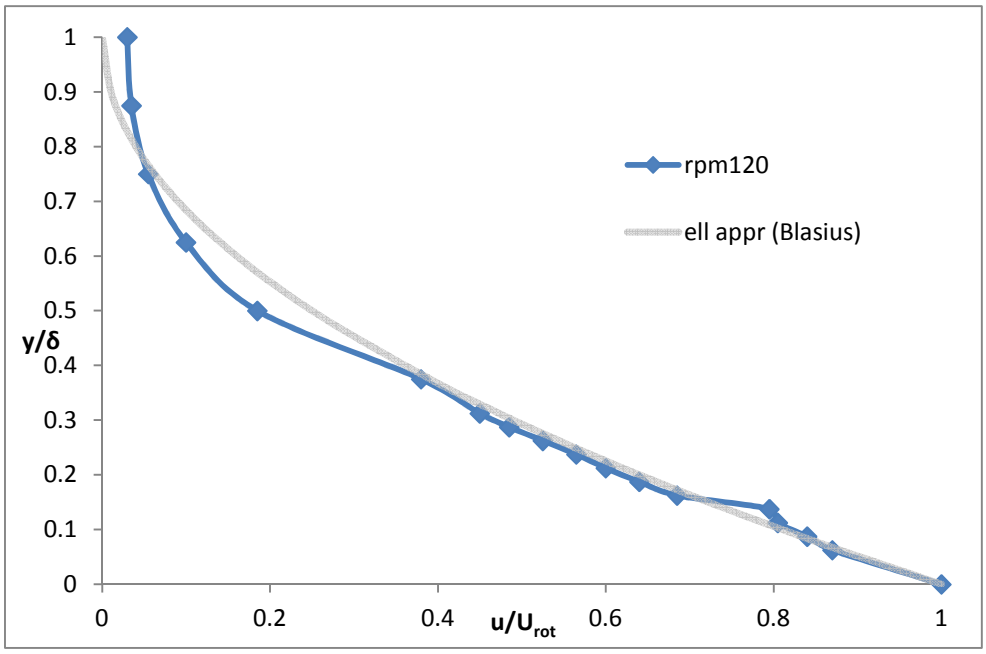

Figure 18 Boundary layer traverse measurement data for the rpm120 (2 m/s) test case

Distribution A: Approved for public release; distribution is unlimited.

This observation is in line with results obtained by Liepmann (1943) [19], who investigated boundary layer profiles at zero pressure gradient conditions within bent wind tunnel test sections of both convex and concave shape, and compared them, to those developing within a straight test configuration. Liepmann (1943) [19] found that the transition mechanisms in the boundary layer over a convex section matched closely to those over a straight configured test section, whereas the concave case was showing considerable deviations. The latter can probably be attributed to Görtler type instabilities developing over concavely formed surfaces [37]. Assuming that similar transition mechanisms necessitate similar boundary layer velocity profiles, comparison to Blasius appears to be viable.

Since the data obtained in this project was subject to some pressure gradient, a somewhat fuller profile when comparing to Blasius could be expected. On the other hand, the inertial forces (which are inherent in this test facility) are likely to counterbalance the effect to some extend by stretching the boundary layer profiles. This finds substantiation by the thicker than normal boundary layers developing when considering the stream-wise distance from the test section inlet to the measurement location.

The data, furthermore, suggests that there is an optimum rotational speed for the current test facility. While the 60 rpm (1 m/s) test case tends to slightly deviate from the Blasius solution, the 180 rpm (3 m/s) profile shape seems to behave like a turbulent boundary layer near the surface which then appears to adapt to the Blasius profile towards the boundary layer edge (see Figure 19).

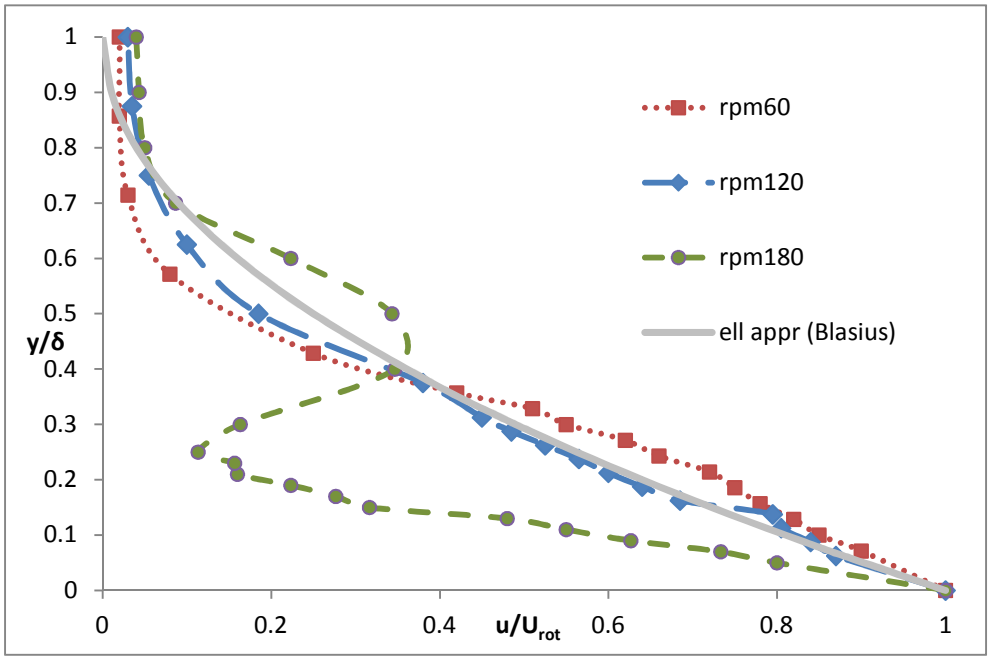

Figure 19 Boundary layer traverse measurement data for several rotational speeds

Distribution A: Approved for public release; distribution is unlimited.

By far the closest match when compared to the Blasius solution was obtained with a 120 rpm (2 m/s) rotational speed. For that reason, it was chosen as the base flow condition for subsequent particle investigations. This speed provides for a Reynolds number of greater than 300 at a distance of about 3 mm above the drum for an object with a diameter of 5 mm. While for investigations on a cylindrical particle this is more than adequate, for those on a spherical one it is considered the absolute minimum.

Furthermore, possible suppression of vortices due to wall proximity as proposed by Zdravkovich (2002) [43] for a circular cylinder would make any location closer to the drum ineligible for the anticipated purpose of this study. These considerations currently restrict possible experiments to objects that meet the above-mentioned dimensions at a single rotational speed.

Therefore, subsequent to preliminary particle experiments, efforts should be undertaken to sufficiently stabilize the flow at higher rotational speeds, in order to widen the window for experimentations.

Hot Wire Measurements

Calibration procedures: Calibrating the HW probes represented another problem for this project. Since in general the calibration procedure needs to be carried out within an undisturbed free stream, the newly developed test facility could not be used, as the current setup makes it impossible to cover the velocity range required for the boundary layer measurements. This issue was overcome by conducting the calibration process in another wind tunnel located in the same laboratory. Even though this tunnel was not particularly well suited for the very low speeds required for the calibration, careful observation of the calibration curve's behaviour and constant screening to standard Pitot tube readings lead to results that could be used with confidence.

However, this made the calibration a time consuming process. It also suggests a future improvement to the design of the test facility, by adding an additional flow supply.

Technical difficulties encountered: First attempts on taking HW measurements in order to gain more detailed data were unsuccessful in producing conclusive results. Subsequent in-depth post-processing of the single traces revealed high amplitude disturbances near the drums surface, that were quite similar in shape to that known from turbulent spots (see Figure 20). These distortions were exactly in line with the rotational speed of the drum, thus indicating that a slight concentricity deviation of the drum was causing the issue. Earlier measurements using a micrometer gauge had shown the drum being out of centre by approximately 50 µm (a distance that had been considered sub-critical at the chosen speeds until then.

Distribution A: Approved for public release; distribution is unlimited.

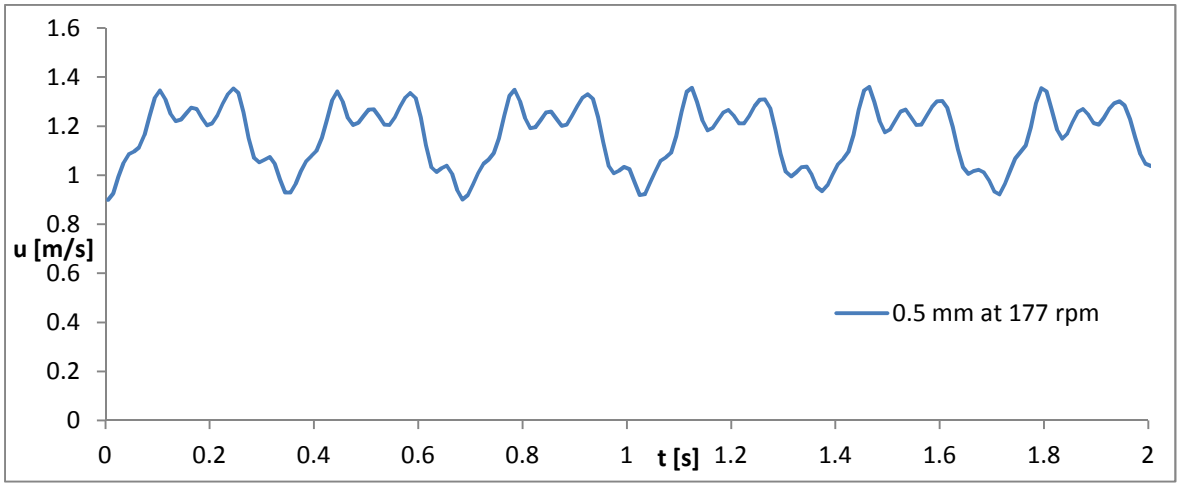

Figure 20 Disturbances recognized in the HW signal before improving the drum's concentricity

In order to not lose the facilities very good balancing, which was reflected by a nearly vibration-free operation throughout the entire required speed range, the decision was made to correct the concentricity in-situ without disassembly of any part that was driving the drum. This has been accomplished by coating the drum with an easy to "sand" filler (Isopon P38 Easy Sand), which after sufficient hardening has been ground down by using a very fine grade sand paper that was glued to a perfectly straight edge covering the whole width of the drum. Clamping this purpose-made tool squarely to the frame of the facility such that it just touched the highest point of the drum and slowly rotating the latter, took material off only in the required region until no frictional noise could be heard for a full rotation. The procedure was carefully repeated until the initial friction of the sandpaper occurred uninterruptedly throughout a full turn of the drum.

Subsequent to the above described modification, no movement of the shading image of an object located close to the drum's surface could be observed by the naked eye. Successive measurement revealed that the procedure had succeeded to reduce the concentricity deviation to as little as 5 µm, while at the same time improving the surface smoothness and entirely preventing any surface rust accumulation.

Unfortunately, as is apparent from the subsequently repeated HW measurements, this was still insufficient to eliminate the previously observed distortions (see Figure 21). While the spot-like nature of the disturbances had disappeared, their amplitude was still very large. However, the latter diminished with wall-normal distance and seemed to have completely dampened above the boundary layer edge as determined by preceding Pitot traverses, thus supporting the derived value of the boundary layer thickness (see Figure 22).

Distribution A: Approved for public release; distribution is unlimited.

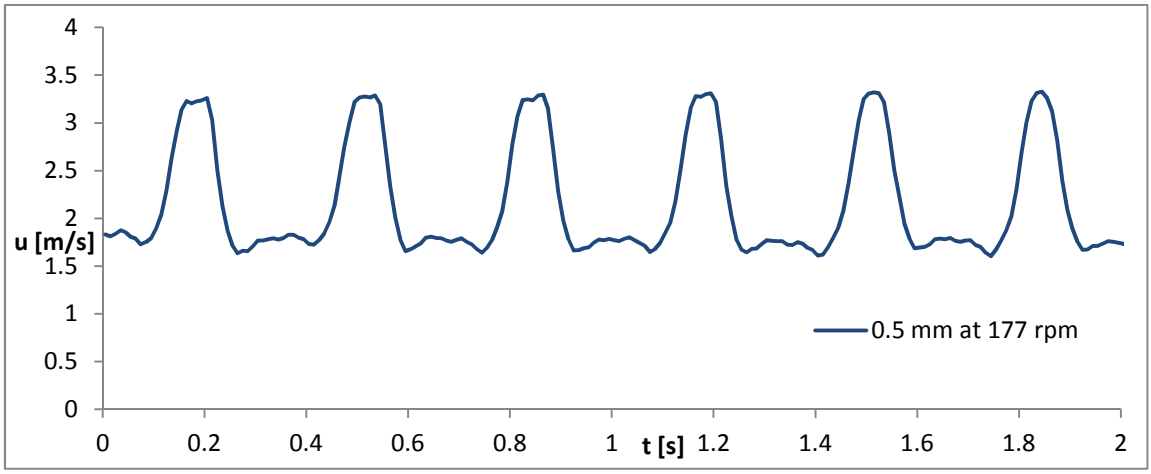

Figure 21 Disturbances recognized in the HW signal subsequent to improving the concentricity

Figure 22 also illustrates that the structure of the disturbance changes within the boundary layer. While near the surface as well as towards the boundary layer edge the signal shows a quite smooth wave-like appearance, a more spiky deflection of larger amplitude is found in the central regions of the boundary layer. Apparently, the proximity of both, the surface and the nearly quiescent free stream, tends to dampen distortions for the chosen test case.

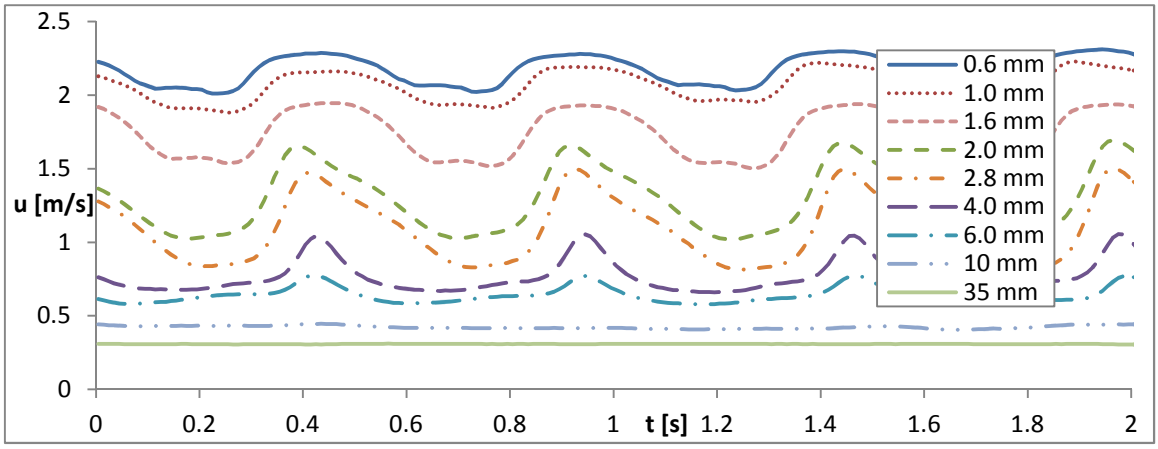

Figure 22 Disturbances as measured by HW throughout a boundary layer traverse at rpm 120 subsequent to reducing the concentricity deviation

Investigating measurement results obtained at locations further away from the wall reveals the importance of the achieved concentricity improvements. Whereas the post-modification data shows no evidence of the surface imperfection outside the boundary layer, the pre-modification flow field was still strongly affected at a wall normal distance of 35 mm (see Figure 23). Furthermore, the latter signal appears to be quite irregular, which indicates that the underlying boundary layer was certainly not laminar in this case.

Distribution A: Approved for public release; distribution is unlimited.

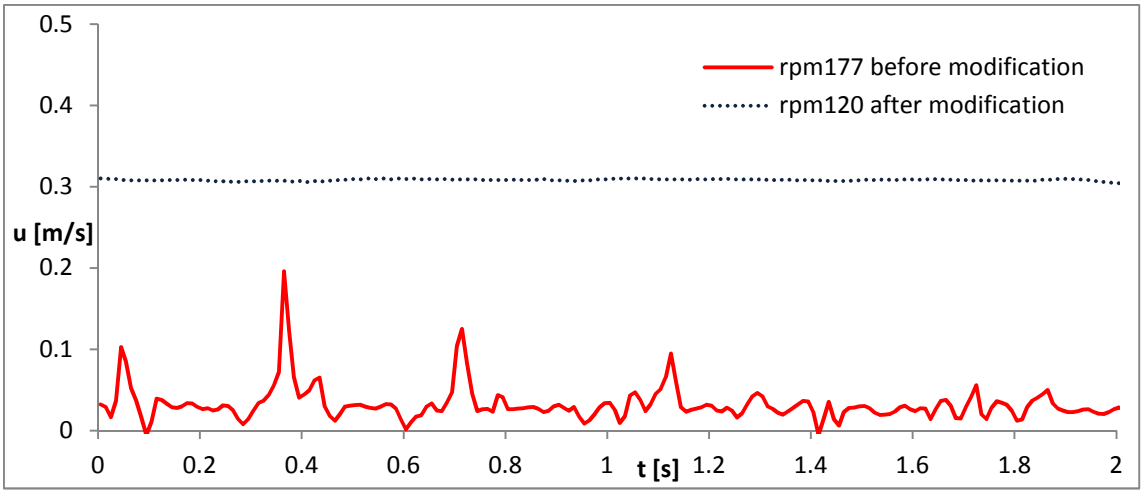

Figure 23 Comparison of hot HW signals at a distance of 35 mm normal to the drum's surface before and subsequent to reducing the concentricity deviation

This is unlike all traverse data shown in Figure 22, which reminds in appearance of Tollmien-Schlichting (TS) waves [35], a disturbance type that is known to be tolerable by a laminar boundary layer to a certain extend without causing a breakdown to turbulence.

It must be noted that the data shown for the 177 rpm test case provided in Figures 22 and 23 was subject to an initial calibration problem and thus only amounts to about half its actual value. Since the above considerations are dealing with the signals' structural influence onto the flow field this is seen to be of no relevance at this point.

Discussion of measurement results obtained from Boundary Layer traverses

A further finding of the above described laboratory studies is that the boundary layer thickness seems to slightly increase with speed. While at a rotational speed of 1 m/s a delta, δ, of 7 mm was determined; at 2 m/s this had increased to about 8 mm. At 3 m/s all indication pointed towards a delta of 10 mm. However, it must be noted that the shape of the latter boundary layer profile is showing some near wall turbulent structures.

This behaviour could be explained by the higher energy of the near wall air particles when subjected to a higher rotational speed of the drum due to the no-slip condition. These particles are increasingly likely to carry along air parcels further away from the wall with increasing kinetic energy. This also explains, why the x-value as required for the calculation of eta in the Blasius solution could not simply be taken as the stream-wise distance between test section inlet and measurement location.

Furthermore, it is interesting to observe the peculiar shape of the 3 m/s test case. It seems to suggest that the breakdown of the laminar boundary layer develops gradually from the wall region,

Distribution A: Approved for public release; distribution is unlimited.

before a completely turbulent boundary layer is obtained. However, such statement would require further substantiation from measurements to be taken at higher velocities.

Pressure Transducer Measurements

In order to investigate whether or not the wave-like disturbances indeed stem from wall normal flow components, a pressure transducer has been employed. This has been done, since on one hand it would only detect flow changes in the anticipated (stream-wise) direction while on the other it provides for readings that are of high frequency, and thus (unlike a standard manometer) enables for the detection of the observed disturbances, if they were to act in this direction.

An example measurement taken at 2 m/s rotational speed at 1 mm and at 4 mm above the wall is illustrated in Figure 24. It is evident that the distortions found in the HW signals did not occur here. Since the pressure transducer could only sense flow fluctuations in the stream-wise direction, it can be stated that these low-frequency high-amplitude disturbances, originate exclusively from wall-normal imperfections.

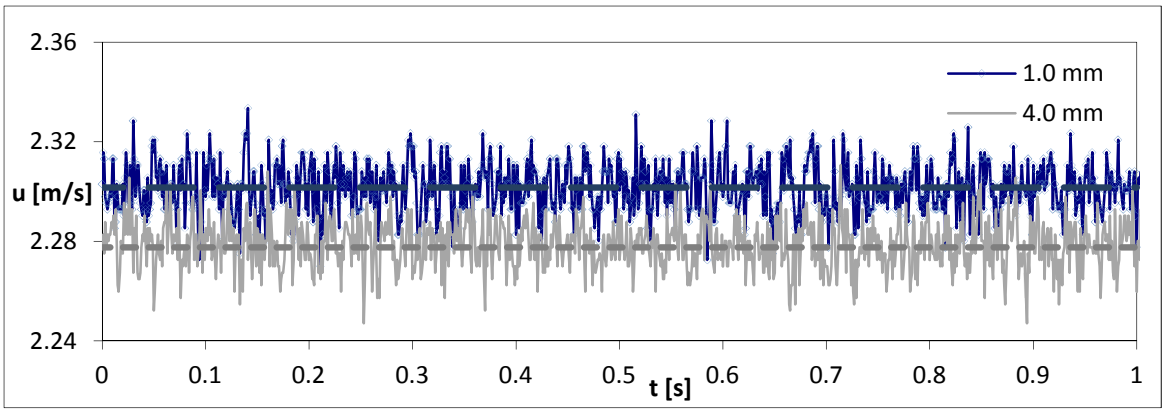

Figure 24 Near wall measurements using a pressure transducer at a sampling rate of 5 kHz, clearly not showing any regular low frequency disturbances of high amplitude

Unfortunately, even though a high spec transducer has been acquired, its sensitivity was insufficient to allow for complete boundary layer traverses. Nevertheless, the findings of Figure 24 give confidence that application of a crossed wire probe could resolve the issues initially encountered when attempting to obtain results from HW measurements, since such a probe can resolve both the x- and the y-component of a velocity vector independently.

Distribution A: Approved for public release; distribution is unlimited.

Smoke Flow Visualisation

Since there was little known about the flow field developing within the test section of the facility built during this project, supporting application of flow visualisation techniques was considered essential.

While initially oil based smoke was considered for its easy and cost effective generation and its white colour, which is stated to be most suited for visualization purposes [36] , the problem of severe oil condensation in the test section has led to the decision of employing a dry combustion based technique instead. An oil film, coating the drum, was believed to introduce large errors to the developing flow field by upsetting the no slip condition of air particles at the drum's surface. While cigarette smoke would have been the preferential solution on the above stated grounds, this could not be used for legal reasons. Thus, the final choice was made for using incense in combination with a sufficiently strong green light laser (15mW, class 1M), that could be focussed to illuminate a thin sheet. The most important of in that way obtained results are illustrated within Figures 25 to 28.

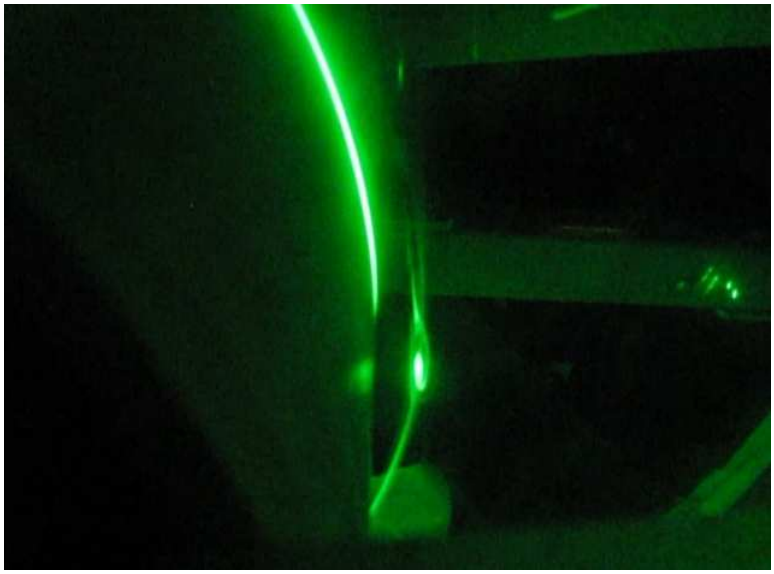

Figure 25 Steady vortex developing at the boundary layer edge half way through the test section at zero pressure gradient conditions

Since the theory for a thin flat horizontal plate of infinite dimensions suddenly set into motion horizontally proposed that all flow above its surface will gradually take on the speed of the plate with time passing [30], the facility had been designed to work against the gravitational force, in order to possibly counterbalance the effect to some extent. However, the development of a steady vortex near the boundary layer edge and in particular its orientation (see Figure 25) gave room for the speculation that this could be a result of gravity thwarting the kinetic energy of the flow which is swept along with

Distribution A: Approved for public release; distribution is unlimited.

the drum's surface. This would also explain the location of the vortex near the point where the effect may be strongest, at about half way through the test section.

Even though this vortex could be shifted further downstream by diffuser modifications as described in an earlier section, it proved difficult to achieve regions lying behind the initially anticipated measurement location, as is apparent from Figure 26. Hence, it was decided to position all subsequent measurements a few degrees further upstream, in order to be not dependent on the introduction of considerable pressure gradients.

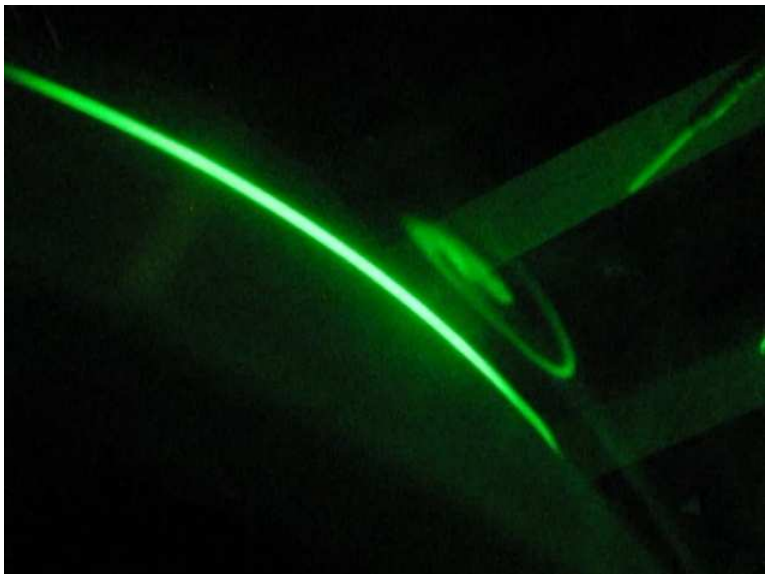

Figure 26 Steady Vortex shifted downstream by partially blocking the diffuser exit; however, this is near the initially anticipated measurement location

Please note within Figure 26, the clear region upstream of the vortex, adjacent to the drum's surface that is bound by a thin streak of smoke. This is believed to represent the developing boundary layer since in here the smoke is carried away quickly due to the higher speed of the air particles. The width of this region agrees well to the earlier from traverse data derived boundary layer thickness.

Even though slight pressure modifications and relocation of the measurements were successful in providing a stable flow condition for the subsequent particle studies, it should also be investigated, whether or not reversing the drum's rotational direction would overcome the issues that may be connected to gravitational forces (please note that the test facility had been designed from the beginning to allow for interchanging the in- and outflow conditions without great efforts).

Surprisingly, the smoke being delivered from the diffuser side this time still appeared to be rising. Unfortunately, the visualisation capabilities were unacceptably reduced. Thus, the smoke introduction was moved back to the contraction side (representing the outflow for this study), which considerably improved the obtainable views.

Distribution A: Approved for public release; distribution is unlimited.

As a first important result, the incense smoke (being of higher temperature than the ambient air) was free to rise within the free stream, making apparent a nearly quiescent flow within this region, even at higher rotational speeds of the drum. Secondly, as illustrated in Figure 27, the flow structures of the rising incense were rapidly swept along (downwards) when coming close to the drum's surface, again providing for an approximate indication of the existing boundary layer thickness. A steady vortex could not be observed at any location near the boundary layer edge. However, obtained illustrations appeared somewhat less conclusive than in the anti-clockwise rotating case, since irregular smoke patterns developed throughout the free stream while overlaying the flow features being of greater interest for this particular project.

Figure 27 Flow structure of within the free stream rising incense being swept along with the boundary layer over the reversely (clockwise) rotated drum

In summary, employing the clock-wise rotating approach would lose a lot in terms of smoke flow visualisation and possibly increase the overall turbulence level within the free stream due to the smoke rising against the background flow generated by the drum's rotation. Hence, the decision was made to adhere to the initial setup, unless more severe difficulties should occur. Figure 28 shows the stable flow condition achieved at the location, where subsequent particle impact analysis will take place.

Unfortunately, while providing quite clear and steady illustrations of the flow within the free stream, the smoke within the area of interest, namely within the boundary layer, is carried away quickly making it somewhat more difficult to capture developing flow structures in here.

Distribution A: Approved for public release; distribution is unlimited.

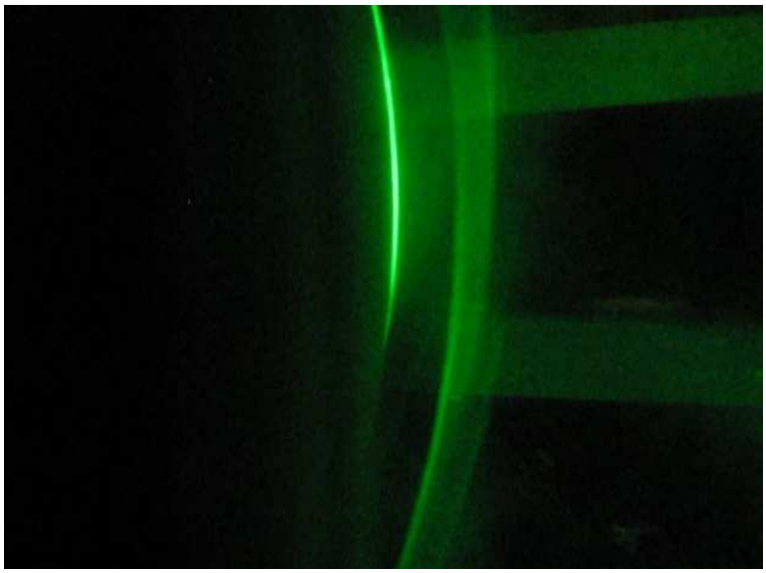

Figure 28 Stable flow at the anticipated measurement location

The impact of a particle on the laminar boundary layer- Part 1

In order to surmount the problem of a practically smoke-free boundary layer, an attempt was made to entrain the incense directly from the particle itself. This has been achieved by attaching the particle to a capillary tube, which was connected to the smoke reservoir. The latter consists of a large syringe which is filled with incense before each experiment and also serves to provide for the pressure required to entrain the smoke through a little hole in the particle. In order to avoid additional disturbances, the jet containing the smoke must be kept at a very low speed, which was found to be easily controllable.

Figure 29 shows an example illustration of a streak of smoke initiated from a spherical particle (d = 6 mm) located about 2.5 mm above the drum, which was rotating at 120 rpm. Apparently, there is no sign of a developing vortex despite of a sufficiently large Reynolds number. It seems that the flow drawn with the rotational drum completely counteracts any vortex development from the wall adjacent particles surface. Whether or not this involves turbulence being produced in the boundary layer behind the immersed particle is currently not known. In other words, if the particle is positioned at a wall normal distance that is smaller than a certain critical value, which needs to be specified, then the vortex that would normally start rolling in towards the particles centre line within the near wake is stretched by the faster moving surrounding flow before it can form. Since the side of the particle furthest away from the drum is subcritical, this would mean that the wake development as known from theory for a uniform flow field is completely suppressed for the illustrated case.

Distribution A: Approved for public release; distribution is unlimited.

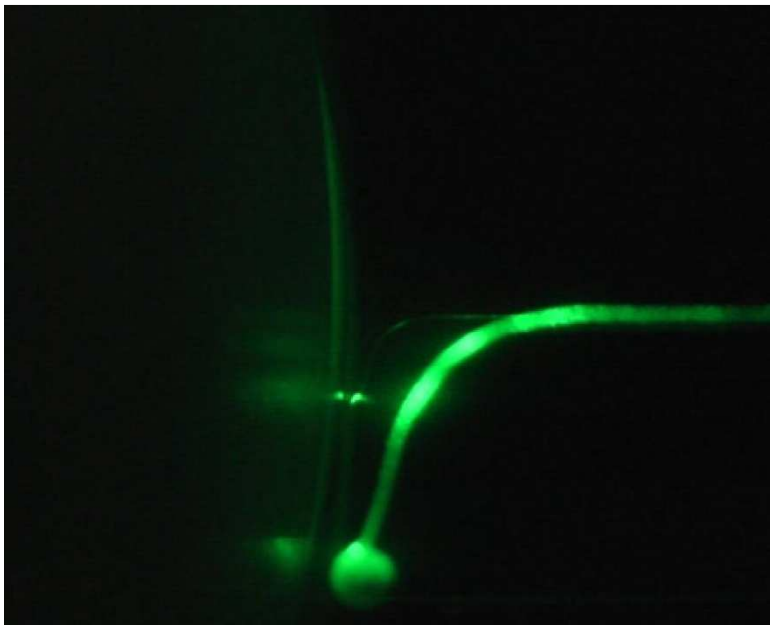

Figure 29 Thin streak of smoke entrained from a spherical particle and drawn along with the rotational drum at rpm 120.

Thus in this region turbulence can only occur if the disturbance excites within the boundary layer and breaks down into a turbulent spot some distance downstream of the particle, or if the particle is large enough for transition to occur on its surface before the wake detaches.

Unfortunately, this was the only configuration providing for illustrations that were sufficiently clear to allow for video images to be taken. Please note that only the lower right illustration within Figure 29 represents the actual particle, while all other appearing objects are a result of optical reflections from both the test section side wall and the rotational drum.

Work in progress

Flow field definition

The issues encountered when using single HW probes have led to the decision to employ X HW cross flow probes instead. This will result in a clearer definition of the flow field provided by the alternative experimental approach described herein. The flow definition explorations will be made at different locations and rotational speeds and also be repeated at several times after running up the test facility. Whereas, the latter will rule out or not any time dependence, the former should indicate whether or not self-similarities between the profiles can be achieved, as can be observed in zero pressure gradient flat plate boundary layers.

Distribution A: Approved for public release; distribution is unlimited.

The impact of a particle on the laminar boundary layer- Part 2

The limitations inherent to the currently applied smoke flow visualization technique and the problems encountered during HW single probe measurements have as yet prevented the reliable determination of a critical particle Reynolds number.

This makes an upgrade of the applied measurement technique a requirement. Particle Image Velocimetry (PIV) is believed to satisfactorily overcome encountered issues if sufficient seeding of tracer particles into the boundary layer, which develops over the rotational drum, can be achieved.

Also, the double (or so-called "raised") Pitot approach is under consideration as a supplementary technique, since it has proven to successfully work during flight tests [6], and also in the laboratory [31]. However, due to the low speeds inherent to the setup of the test facility, the earlier used equipment failed to detect reliable readings. Unfortunately, the higher-spec pressure transmitter (0-0.1 mbar) that has been sourced for this purpose could not be made available in time.

Considering the small window available for measurements on a spherical object, also cylindrical particles will be included in all subsequent investigations. This will furthermore allow for a more direct comparison to the "Hall criteria" [9]. The particles will be fixed at both sub- and supercritical conditions within the established non-uniform flow field at several elevations above the drum. The investigation of the particle wakes, forming under these conditions, should reveal the critical parameters, above which turbulence is produced in a wake.

With regard to this and the preceding section there will be an amendment to this report as soon as the corresponding results are available.

Modifications of the test facility

The test facility, being to the author's knowledge the first of its kind, must be considered a prototype. Hence, it was subject to continued modifications, the requirement of which arising from lessons learnt during its development and initial testing. Furthermore, working on a prototype always leaves room for the emergence of new ideas that would lead to performance improvements, some of which are proposed within this section.

The experiences acquired while working on the test rig has indicated that it may be advisable to introduce additional flow to the test section. The advantages could be twofold. On the one hand, the kinetic energy of the free stream produced in that way could improve the overall flow stability near the boundary layer edge. On the other hand, the test facility could be set to the specific needs of a particular experiment, making it, for instance, possible to also investigate an object of 2 mm diameter further away from the wall. This could be set by carefully adjusting both free stream speed and a respectively higher velocity of the rotational drum. Such a modification would, of course, require an

Distribution A: Approved for public release; distribution is unlimited.

upgrade of the current system used to rotate the drum, since rotational capabilities of up to 600 rpm (or more) might be necessary. Furthermore, the employment of a stepper motor would be beneficial allowing for constant rotational speeds to be set from a computer.

Due to the fact that flow within the settling chamber is barely existent in the current setup, only a simple design in terms of flow straightening and conditioning was required. However, when introducing additional flow supply, a more complex approach has to be considered, in order to provide for a sufficiently disturbance free environment of low turbulence within the test section. This can be achieved by a properly designed combination of honeycomb and turbulence grids to be implemented into the inlet of the settling chamber. In this way, any flow passing the inlet will be made homogenous and isotropic and be of reduced turbulence intensity before entering the contraction area. A suction type flow supply from the diffuser end is currently considered to be the preferable solution. The above described modifications are currently underway.

Surprisingly, even at the very low test speeds, already the tiniest derivations from concentricity seem to cause great difficulties when attempting high quality HW measurements. Thus, the central part of the facility, namely the rotational drum, would need to be upgraded by a construction similar to one being generally applied to high quality bearings, in order to improve the flow quality above that which can be obtained by the current prototype test rig.

Conclusions

(1) The published information on the mechanisms leading to the transition of a laminar boundary layer due to a small particle travelling through it is incomplete.

(2) The critical parameters above which transition is triggered within the affected laminar boundary layer have not been experimentally verified prior to the current study.

(3) Conventional laboratory methods are not likely to capture all facets of the naturally occurring mechanisms without appreciable efforts requiring access to the latest state-of-the-art measurement techniques. An alternative method, which is described in detail within this document, has been shown to be viable.

(4) A computational pre-study on the alternative experimental method has resulted in time-limited boundary layer growth and a stable non-uniform flow field.

(5) The proof of concept of the alternative experimental approach was demonstrated by actual experimentation. The new test facility has been proven to provide for a stable non-uniform wall-bounded flow field.

(6) The results of both the CFD study and the preliminary experiments indicate thicker than normal boundary layers when compared to flat plate solutions.

Distribution A: Approved for public release; distribution is unlimited.

(7) The level of observed background flow found in the “free stream” is low, and particles can easily be kept at subcritical conditions within this region.

(8) The level of observed background flow can be considerably reduced by applying a flap to the diffuser outlet, thus by introducing a small pressure gradient.

(9) The boundary layer traverse of a flattened miniature Pitot tube resulted for a specific frequency of the rotating surface in a velocity profile that provided a surprisingly close match when compared to the Blasius profile. Since this speed also allows for a comprehensive particle investigation it has been defined as the “optimal configuration”.

(10) Already very small concentricity deviations of the rotational drum were seen to have a large effect onto results as obtained from HW measurements. While the effort to improve the found concentricity deviation was successful in reducing the effect to within the boundary layer the disturbances in here persisted rendering single HW probes ineligible for producing useful results.

(11) Smoke flow visualization on a particle immersed into the boundary layer indicates that there exists a region within which the development of a particle wake could be completely suppressed.

(12) Meaningful visualizations of the particle’s wake when immersed into the non-uniform flow field of the boundary layer proved to be difficult, since the smoke within the latter is carried away too quickly to allow for video images.

(13) Outside of those regions the applied technique provided for clear representations, substantiating both a “quasi-quiescent free stream” and the boundary layer thickness as derived from Pitot traverses.

(14) An upgrade of the currently applied measurement techniques in terms of X HW cross flow probes and PIV is seen to be a requirement, in order to establish the desired critical particle parameters.

Acknowledgement

Effort sponsored by the Air Force Office of Scientific Research, Air Force Material Command, USAF, under Grant number FA8655-11-1-3044. U.S Government is authorized to reproduce and distribute reprints for Governmental purpose notwithstanding any copyright notation thereon.

Distribution A: Approved for public release; distribution is unlimited.

List of Symbols, Abbreviations, and Acronyms

Symbols

a	speed of sound
A	cross sectional area
c	contraction ratio
d	diameter
G	transverse velocity gradient
h	normalized height
H	height
K	local shear parameter
L	length
l	length
Ma	Mach number
Re	Reynolds number
St	Strouhal number
u	stream-wise velocity
U	stream-wise velocity
t	time
x	coordinate in stream-wise direction
y	coordinate in transverse direction

Subscripts

crit	referring to a critical condition
i	inlet
e	exit
o	outlet
p	referring to a particle
rot	referring to a rotational movement
x	in stream-wise direction
y	in transverse direction
∞	referring to conditions at infinity

Distribution A: Approved for public release; distribution is unlimited.

Greek

δ	boundary layer thickness
η	auxiliary variable
θ	cone angle
υ	dynamic viscosity
ξ	normalized length

Abbreviations and Acronyms

BC	Boundary Condition
CFD	Computational Fluid Analyses
DVB	DiVinylBenzene
HW	Hot Wire
LFC	Laminar Flow Control
NASA	National Aeronautics and Space Administration
NI	National Instruments
PIV	Particle Image Velocimetry
R & D	Research and Development
rpm	rotations per minute
SAS	Simulated Airline Service
TS	Tollmien-Schlichting
TSI	Thrust. Science. Innovation.
US	United States
USAF	United States Air Force

Distribution A: Approved for public release; distribution is unlimited.

References

[1] Arnal, D. & Archambaud, J.P. Laminar-Turbulent Transition Control: NLF, LFC, HLFC, *AVT 151 Lecture Series on Advances in Laminar-Turbulent Transition Modelling*, June 9-13, 2008, von Karman Institute for Fluid Dynamics, Brussels.

[2] Barker, S.J. & Gile, D. Experiments on heat stabilized laminar boundary layers, *J. Fluid Mech.*, Vol. 104, 1981, pp. 139-159.

[3] Bell, J. H., Metha, R. D. Boundary Layer Predictions for Small Low-Speed Contractions, AIAA Journal, Mar 1989, Vol. 27, No. 3, pp. 372-374.

[4] Brassard, D., Ferchichi, M. Transformation of a Polynomial for a Contraction Wall Profile, ASME, J. of Fluid Eng., Jan 2005, Vol. 127, pp. 183-185.

[5] Davis, R.E., Maddalon, D.V., Wagner, R.D. Performance of Laminar Flow Leading Edge Test Articles in Cloud Encounter, NASA CP-1987-2487, Langley Research Center, 1987.

[6] Davis, Richard E. et al., (1989), "Evaluation of Cloud Detection Instruments and Performance of Laminar-Flow Leading-Edge Test Articles During NASA Leading-Edge Flight-Test Program", *NASA/TP-1989-2888, Langley Research Center, Hampton, Virginia, USA.*

[7] Doolan, C. J. Numerical Evaluation of Contemporary Low-Speed Wind Tunnel Contraction Designs, ASME, Technical Note, J. of Fluid Eng., Sep 2007, Vol. 129, pp. 1241-1244.

[8] Fowell, L.R. & Antonatos, P.P. Some Results from the X-21A Program, AGARDograph, Part I, Recent Developments in Boundary Layer Research, May 1965

[9] Hall, G.R. On the Mechanics of Transition Produced by Particles Passing Through an Initially Laminar Boundary Layer and Estimated Effect on the Performance of X-21 Aircraft, Northrop Corp., Contract-No.: N79-70656, 1964.

[10] Hall, G.R. Interaction of the wake from bluff bodies with an initially laminar boundary layer, AIAA Journal, V. 5, No. 8, pp. 1386-1392, 1965.

[11] Hall, G.R. Interaction of the wake from bluff bodies with an initially laminar boundary layer, AIAA-1966-126, *Aerospace Sciences Meeting*, 3rd, New York, N.Y., Jan 24-26, Paper 66-126, 1966.

[12] IATA, Airline & Operations, *Fuel Conservation*, accessed online, 29th July 2011, http://www.iata.org/whatwedo/aircraft_operations/fuel/pages/fuel_conservation.aspx.

[13] Jasperson, W.H., Nastrom, G.D. GASP Cloud Encounter Statistics: Implications for Laminar Flow Control Flight, *Journal of Aircraft*, Vol. 21, No. 11,1984, pp. 851-857.

[14] Jasperson, W.H., Nastrom, G.D., Davis, R.E., Holdeman, J.D. Variability of Cloudiness at airline Altitudes from GASP Measurements, *Journal of Climate and Applied Meteorology*, Vol. 24, 1985, pp. 74-82.

Distribution A: Approved for public release; distribution is unlimited.

[15] Ladd, D.M. & Hendricks, E.W. The effect of background particulates on the delayed transition of a heated 9:1 ellipsoid, *Exp. in Fluids*., V. 3, 1985, pp. 113-119.

[16] Lauchle, G.C. & Gurney, G.B. Laminar Boundary Layer Transition on a Heated Underwater Body, *J. Fluid Mech*., V. 144, 1984, pp. 79-101.

[17] Lauchle, G.C., Petrie, H.L., Stinebring, D.R. Effects of Particulates on the Delayed Transition of a Heated Body, Applied Research Laboratory Technical Memorandum 86-213, 1986.

[18] Lauchle, G.C., Petrie, H.L., Stinebring, D.R. Laminar Flow Performance of a Heated body in particle-laden water, *Exp. in Fluids*, Vol. 19, 1995, pp. 305-312.

[19] Liepmann, H. W., Investigations of Laminar Boundary Layer Stability and Transition on Curved Boundaries, NACA ACR 3H30, USA, 1943.

[20] Loth, E. *Computational Fluid Dynamics of Bubbles, Drops and Particles*, University of Illinois at Urbana-Champaign, Draft for Cambridge University Press, Jan. 2007, http://www.ae.uiuc.edu/~loth/CUP/Loth, accessed on May, 9th 2007.

[21] Maddalon, D.V. & Braslow, A.L. Simulated-Airline-Service Flight Tests of Laminar-Flow Control with Perforated-Surface Suction System, NASA TP-2966, Langley Research Center, 1990.

[22] Metha, R. D., Bradshaw, P. Design rules for small low speed wind tunnels, Aero. Journal, Nov 1979, Vol. 73, pp. 443-449.

[23] Mochizuki, M.V. Smoke Observation on Boundary Layer Transition Caused by a Spherical Roughness Element, *J. Phys. Soc. of Japan*, Vol. 16, No. 5, pp. 995-1007.

[24] Petrie, H.L., Morris, P.J., Bajwa, A.R., Vincent, D.C. Transition induced by Fixed and Freely Convecting Particles in Laminar Boundary Layers, 1993, The Pennsylvania State University, Appl. Res. Lab., PA, USA.

[25] Pfenninger, W. Design Considerations of Long-Range and Endurance LFC Airplanes with Practically All Laminar Flow, NASA Joint Institute for Advancement of Flight Sciences, Aug. 1982.

[26] Rae, W. H. Jr., Pope, A. *Low-Speed Wind Tunnel Testing*, John Wiley & Sons, USA, 1984.

[27] Roshko, A. On the Development of Turbulent Wakes From Vortex Stresses, NACA TR-1191, Langley Research Center, 1954.

[28] Sakamoto, H. & Haniu, H. A Study on Vortex Shedding From Spheres in a Uniform Flow, *J. Fluid Eng*., V. 112, ASME, 1990, pp. 386-392.

[29] Sakamoto, H. & Haniu, H. The formation mechanism and shedding frequency of vortices from a sphere in uniform shear flow, *J. Fluid Mech*., V. 287, 1995, pp. 151-171.

[30] Schlichting, H. *Boundary Layer Theory*, 7th Edition, McGraw-Hill Book Company, 1979.

Distribution A: Approved for public release; distribution is unlimited.

[31] Schmidt, C. & Young, T.M., The impact of Cirrus Cloud on Laminar Flow Technology, *7th AIAA Aviation technology, Integration and Operations Conference* (ATIO), 18-20 Sep, Belfast, Northern Ireland, 2007.

[32] Schmidt, C. & Young, T.M., The impact of freely suspended particles on laminar boundary layers, *47th AIAA Aerospace Sciences Meeting* (ASM), 5-8 Jan, Orlando, Florida, USA, 2009.

[33] Schmidt, C., Young, T.M., Benard, E.P., Atalay, S. The influence of cirrus cloud on drag reduction technologies based on laminar flow, *CEAS/KAT net II Conference on Key Aerodynamic Technologies*, 12-14 May, Bremen, Germany, 2009.

[34] Schrauf, G. & Kühn, W. Future Needs and Laminar Flow Technology, *Air & Space Europe*, No.3/4, Vol. 3, May-Aug 2001, pp. 98-100.

[35] Schubauer, G. B., Skramstad, H. K. Laminar-Boundary-Layer Oscillations and Transition on a Flat Plate, NACA Rep. 909, USA, 1948.

[36] Szarko, D. J. Smoke-Wire Visualization of an Oscillating Flow in a Gas Spring, Bachelor Thesis, Massachusetts Institute of Technology, USA, 1993.

[37] Tani, I. Production of Longitudinal Vortices in the Boundary Layer along a Concave Wall, *J. of Geophys. Res.*, Vol. 67, No. 8, July 1962.

[38] Vincent, D.C. Transition induced by Fixed and Freely Suspended Spherical Particles in Laminar Boundary Layers, Master thesis, Aerospace Engineering Department, The Pennsylvania State University, 1993.

[39] White, F.M *Fluid Mechanics*, Mcgraw-Hill College, 4th edition, December 1998.

[40] Young, T.M. and Fielding, J.P. Flight Operational Assessment of Hybrid Laminar Flow Control (HLFC) Aircraft Aerodynamic Drag Reduction Technologies. *Proceedings of the CEAS/DragNet European Drag Reduction Conference*, Jun 19-21, 2000, Potsdam, Germany. Edited by Peter Thiede. ISBN 3-540-41911-0. Published by Springer-Verlag, Berlin, 2001, p.99.

[41] Young, T.M. and Fielding, J.P. Potential Fuel Savings due to Hybrid Laminar Flow Control under Operational Conditions, *Aeronautical Journal*, Vol. 105 (1052), 2001, pp. 581-588.

[42] Young, T.M., Brown, P.R.A., Fielding, J.P. The Impact of Cloud Encounter on Hybrid Laminar Flow Control Aircraft Operations, *CEAS Aerospace Aerodynamics Research Conference*, Cambridge, Paper 58, 10-12 June 2002.

[43] Zdravkovich, M. M. *Flow Around Circular Cylinders Volume 2: Applications*, Oxford University Press, USA, 2002.

Distribution A: Approved for public release; distribution is unlimited.

Finances

Table 1 List of Finances (currency conversion based on 01.09.2011 for 1st rate and on 01.03.2012 for 2nd rate; 1st rate applied for expenses until amount was exceeded)

in/out	in Dollar	in Euro	Item	Date
incoming	15,000.00 $	10,275.00 €	Grant FA8655-11-1-3044 (1st rate) exchange rate: 1.46	01.09.2011
	10,000.00 $	7,505.00 €	Grant FA8655-11-1-3044 (2nd rate) exchange rate: 1.33	01.03.2012
expenses	1,240.87 $	850.00 €	personnel Sep 2011	25.09.2011
	1,240.87 $	850.00 €	personnel Oct 2011	25.10.2011
	1,240.87 $	850.00 €	personnel Nov 2011	25.11.2011
	1,240.87 $	850.00 €	personnel Dec 2011	29.12.2011
	1,240.87 $	850.00 €	personnel Jan 2012	25.01.2012
	1,240.87 $	850.00 €	personnel Feb 2012	25.02.2012
	1,240.87 $	850.00 €	personnel Mar 2012	25.03.2012
	1,240.87 $	850.00 €	personnel Apr 2012	25.04.2012
	1,240.87 $	850.00 €	personnel Jun 2012	25.06.2012
	1,240.87 $	850.00 €	personnel Jul 2012	25.07.2012
	1,459.85 $	1,000.00 €	study fees	in progress
	433.56 $	297.00 €	power supply	cancelled, loan extended
	1597.93 $	1199.25 €	TSI HW probes 1201-6, probe holder 1150-6, shipping	05.04.2012
	729.93 $	500.00 €	TSI standard X HW 1240-T1.5	ordered
	0.00 $	0.00 €	Pitot probe	cancelled, loan extended
	0.00 $	0.00 €	Manometer	cancelled, loan extended
	0.00 $	0.00 €	Shell ondina oil smoke	cancelled, not suitable
	561.85 $	421.67 €	Picotronic focusable line laser LC532-15-5-F, mount, power supply, shipping	02.05.2012
	452.67 $	310.08 €	National Instruments Data Acquisition Card NI PCI-6220, shipping	04.05.2012
	185.80 $	139.49 €	Motor Hawk Controller Card, Stepper Motor, shipping	18.06.2012
	195.19 $	146.49 €	DigiKey Pressure Transducer 442-1011-ND	08.07.2012

Distribution A: Approved for public release; distribution is unlimited.

in/out	in Dollar	in Euro	Item	Date
	1,196.40 $	897.90 €	Manotherm Pressure Transmitter DN51411, shipping	30.07.2012
	3,553.63 $	2,667.00 €	Management overhead, University of Limerick (15%)*	01.08.2012
	1,561.86 $	1174.33 €	Travel cost (AIAA conf./Dayton)	15.09.2012
	1,332.45 $	1,000.00 €	Loan of PIV system (10 working days)	rental agreement in place
Total	-239.17 $	-176.16 €	Please note that some values provided are indicative (and as such the total amount), since work is still in progress (e.g. PIV, X-Wire). A final statement of the corresponding account will be made available in a supplementary report	

*this includes in stock materials & consumables, personnel cost of technicians, and access to publications

Distribution A: Approved for public release; distribution is unlimited.